Productivity, Respiration, and Light-Response Parameters of World Grassland and Agro-Ecosystems Derived From Flux-Tower Measurements

G. Gilmanov Tagir, Vincent Allard, D. Baldocchi, Pierre Béziat, Eric Ceschia, Pierre Cellier, J.F. Soussana

Productivity, Respiration, and Light-Response Parameters of World Grassland and Agro-Ecosystems Derived From Flux-Tower Measurements

Tagir G. Gilmanov[1]

and data contributors[2]:

L. Aires[4], *K. Akshalov*[4], *V. Allard*[4], *C. Ammann*[4], *M. Aubinet*[4], *M. Aurela*[4], *J. Baker*[5], *D. Baldocchi*[4], *J. Balogh*[4], *M. Balzarolo*[4], *L. Belelli*[4], *Z. Barcza*[4], *C. Bernacchi*[4], *C. Bernhofer*[4], *V.S. Baron*[5], *J. Berringer*[4], *P. Beziat*[4], *D. Billesbach*[5], *J. Bradford*[3], *K. Brehe*[5], *N. Buchmann*[4], *E. Ceschia*[4], *P. Cellier*[4], *Shiping Chen*[4], *D. Cook*[4], *C. Corradi*[4], *R. Coulter*[4], *R. Czerny*[4], *E. Dellwik*[4], *A. Detwyler*[5], *H. Dolman*[4], *M. Dourikov*[5], *W. Dugas*[3], *J. Elbers*[4], *W. Emmerich*[3], *W. Eugster*[4], *D. Fitzjarrald*[4], *L. Flanagan*[4], *A. Frank*[3], *J. Fuhrer*[4], *D. Gianelle*[4], *T. Griffis*[5], *T. Gruenwald*[4], *M. Haferkamp*[3], *Guo Haiquang*[4], *N. Hanan*[4], *R. Harding*[4], *L. Haszpra*[4], *M. Heuer*[5], *J. Heilman*[4], *A. Hensen*[4], *S. Hollinger*[4], *A. Jacobs*[4], *D. Janous*[4], *W. Jans*[4], *D.A. Johnson*[3], *M. Jones*[4], *T. Kato*[4], *G. Katul*[4], *G. Kiely*[4], *W. Kutsch*[4], *G. Lanigan*[4], *T. Laurila*[5], *P. Leahy*[4], *S. Li*[5], *A. Lohila*[5], *V. Magliulo*[4], *A. Manzi*[4], *M. Marek*[4], *R. Matamala*[4], *T. Meyers*[4,5], *P. Mielnick*[3], *A. Miyata*[4], *E. Moors*[4], *J. Morgan*[3], *C. Moureaux*[4], *M. Nasyrov*[5], *J. Olejnik*[4], *J. Olesen*[4], *W. Oechel*[4], *C. Owensby*[5], *D. Papale*[4], *C. Pio*[4], *J. Prueger*[5], *A. Raschi*[4], *C. Rebmann*[4], *M. Reichstein*[4], *H. da Rocha*[4], *N. Rogiers*[4], *N. Saliendra*[3], *M.J. Sanz*[4], *K. Schelde*[4], *R. Scott*[4], *P. Sims*[3], *R.H. Skinner*[5], *H. Soegaard*[4], *J.-F. Soussana*[4], *M. Sutton*[4], *A. Suyker*[4], *T. Svejcar*[3], *M. Torn*[5], *Z. Tuba*[4], *S. Verma*[4], *M. Waterloo*[4], *G. Wohlfahrt*[4], *Bin Zhao*[4], *Guangsheng Zhou*[4]

Authors are [1]Associate professor at the Department of Biology and Microbiology, South Dakota State University, Brookings, SAG 304, Box 2207B, SD 57007, USA, and [2]researchers who contributed their data to the [3]USDA-ARS RANGEFLUX data set, [4]FLUXNET La Thuile data set, or [5]WORLDGRASSAGRIFLUX data set.

Research was supported in part by the Science Applications International Corporation, Subcontract # 4400089887 to Gilmanov Research and Consulting, LLP.

Correspondence: Tagir G. Gilmanov, Department of Biology and Microbiology, South Dakota State University, SAG 305, Box 2207B, Brookings, SD 57006, USA. Email: tagir.gilmanov@sdstate.edu

LIST OF SYMBOLS

Latin symbols

A_{max} – maximum gross photosynthetic assimilation (mg CO_2 m^{-2} s^{-1})

CumNEE – cumulative net ecosystem CO_2 exchange (g CO_2 m^{-2})

F_c – net CO_2 flux (mg CO_2 m^{-2} s^{-1}; g CO_2 m^{-2} d^{-1})

GPP – annual gross primary production (g CO_2 m^{-2} yr^{-1})

k_T – coefficient in the exponential equation for respiration temperature dependence $(°C)^{-1}$

L – leaf area index (m^2 m^{-2})

L_{max} – seasonal maximum leaf area index (m^2 m^{-2})

P_d – daytime integral of the net ecosystem CO_2 flux (g CO_2 m^{-2} d^{-1})

P_g – gross photosynthetic assimilation (mg CO_2 m^{-2} s^{-1}; g CO_2 m^{-2} d^{-1})

Q – incoming photosynthetically active radiation (μmol CO_2 m^{-2} s^{-1}; mol CO_2 m^{-2} d^{-1})

Q_a – absorbed photosynthetically active radiation (μmol CO_2 m^{-2} s^{-1}; mol CO_2 m^{-2} d^{-1})

PCPN – atmospheric precipitation (mm d^{-1}, mm yr^{-1})

r_d – daytime ecosystem respiration rate (mg CO_2 m^{-2} s^{-1})

R_d – daytime ecosystem respiration (mg CO_2 m^{-2} s^{-1}; g CO_2 m^{-2} d^{-1})

R_e – total ecosystem respiration (mg CO_2 m^{-2} s^{-1}; g CO_2 m^{-2} d^{-1})

RE – annual total ecosystem respiration (g CO_2 m^{-2} yr^{-1})

RH – air relative humidity (%)

R_n – nighttime ecosystem respiration (mg CO_2 m^{-2} s^{-1}; g CO_2 m^{-2} d^{-1})

R_{net} – net radiation (W m^{-2}; MJ m^{-2} d^{-1})

r_0 – ecosystem respiration rate at temperature T_s = 0 °C (mg CO_2 m^{-2} s^{-1})

r_n – night-time ecosystem respiration rate (mg CO_2 m^{-2} s^{-1})

R_n – nighttime ecosystem respiration (mg CO_2 m^{-2} s^{-1}; g CO_2 m^{-2} d^{-1})

R_{net} – net radiation (W m^{-2}; MJ m^{-2} d^{-1})

T_a – air temperature (°C)

t_r – time of sunrise (h)

t_s – time of sunset (h)

T_s – soil temperature (typically, at 5 cm depth) (°C)

$V_{c,max}$- maximum rate of carboxylation (mg CO_2 m^{-2} s^{-1}))

W_s – volumetric soil moisture (m^3 m^{-3})

Greek symbols

α - apparent quantum yield of gross photosynthetic assimilation (mmol CO_2 mol $quanta^{-1}$)

ε, ε_{ecol} – gross ecological light-use efficiency (mmol CO_2 (mol incident quanta)$^{-1}$)

ε_{phys} – gross physiological light-use efficiency (mmol CO_2 (mol absorbed quanta)$^{-1}$)

λ - latent heat of evaporation (MJ kg^{-1})

θ - convexity (curvature) coefficient of the light-response equation (dimensionless)

ρ_d – diffusion resistance to carbon transport (s m^{-1})

ρ_x – carboxylation resistance to carbon transport (s m^{-1})

ABSTRACT

Grasslands and agroecosystems occupy nearly a third of the land surface area, but their quantitative contribution to the global carbon cycle remains uncertain. We used a set of 316 site-years of year-round net CO_2 exchange (F_c) measurements to quantitatively analyze gross primary productivity, ecosystem respiration, and light-response parameters of extensively and intensively managed grasslands, shrublands/savanna, wetlands, and cropland ecosystems worldwide. Analyzed data set included data from 72 flux-tower sites worldwide partitioned into gross photosynthesis (P_g) and ecosystem respiration (R_e) components using the light-response functions method (Gilmanov et al. 2003, Bas. Appl. Ecol. 4:167-183) from the RANGEFLUX and WorldGrassAgriflux data sets supplemented by data from 46 sites partitioned using the temperature-response method (Reichstein et al. 2005, Gl. Change. Biol. 11:1424-1439) from the FLUXNET La Thuile data set. Maximum values of the apparent quantum yield (α = 75 mmol mol^{-1}), photosynthetic capacity (A_{max} = 3.4 mg CO_2 m^{-2} s^{-1}), maximum daily gross photosynthesis ($P_{g,max}$ = 116 g CO_2 m^{-2} d^{-1}), and gross ecological light-use efficiency (ε_{ecol} = 59 mmol mol^{-1}) of intensively managed grasslands and high-productive croplands exceed those for forest ecosystems, indicating high potential of non-forest ecosystems for uptake and sequestration of atmospheric CO_2. Maximum values of annual gross primary production (8600 g CO_2 m^{-2} yr^{-1}), total ecosystem respiration (7900 g CO_2 m^{-2} yr^{-1}), and net CO_2 exchange (2400 g CO_2 m^{-2} yr^{-1}) for non-forest ecosystems are observed in intensively managed grasslands and high-yield crops, and are comparable or higher than in forest ecosystems (excluding tropical forests). On the average, 80% of the non-forest

sites were sinks for atmospheric CO_2, with mean annual net CO_2 uptake 848 g CO_2 m^{-2} yr^{-1} for intensively managed grasslands and 933 g CO_2 m^{-2} yr^{-1} for croplands. The new flux-tower data indicate the need to revise substantially previous views of grassland and agricultural ecosystems as being predominantly a source of carbon, or having a neutral role, in the regional and continental carbon budgets.

Key Words: gross primary production, ecosystem respiration, net CO_2 flux partitioning, light-response functions method, grasslands, croplands

INTRODUCTION

Quantifying the contribution of various ecosystem types in terms of carbon budget and total continental and global exchange of carbon has been recognized as a fundamental task since the very beginning of the carbon cycle science (Rodin and Bazilevich 1968; Whittaker and Likens 1973; Lieth 1975; Rodin et al. 1975; Olson et al. 1983). While generalizations on the role of forest, wetland, and tundra ecosystems in the global carbon budget have been provided recently, resulting in a general consensus on the contribution to the carbon budget of these ecosystem types (Griffiths and Jarvis 2005; Davidson and Janssens 2006; Birdsey et al. 2007; Bridgham et al. 2007; Tarnocai et al, 2007), there is considerably less agreement with respect to grassland and cropland ecosystems.

Available estimates of carbon budgets at the country or continental levels typically characterize grasslands as weak sinks, or as approaching a carbon-neutral state, while croplands are considered moderate to strong sources of atmospheric carbon (Smith and Falloon 2005; Conant et al. 2007). It should be emphasized, however, that those assessments are not based on direct measurements of carbon exchange, but rather on indirect measures such as biomass and soil organic matter inventories. As a rule, indirect measures involve lumping agricultural fields, where organic matter is produced, with locations (feedlots, harvest processing plants, ethanol facilities etc.) where harvested biomass is transported and utilized.

Although fully justified as initial "zero approximations", indirect measures are fundamentally inadequate as tools for understanding the precise contributions of different land areas to regional CO_2 exchange. In contrast, our objective is to get reliable,

measurement-based estimates of carbon fluxes into and out of the system at the ecosystem scale provided by tower records. According to some authors, corn fields producing good harvests of grain with no soil organic matter loss due to advanced agronomic management, but considered together with ethanol producing plants where this corn is processed, will be viewed as only a small net sinks for atmospheric carbon (Powlson et al., 2005; Farrell et al. 2006) or even as net carbon sources (Patzek et al., 2005). This completely overshadows the fact that the field itself is often a very strong sink for atmospheric CO_2 (e.g., Buyanovsky and Wagner, 1998; Hollinger et al. 2005).

The last decade has been characterized by an explosive growth in number and duration of observations from nonforest flux tower stations all over the world. Through the La Thuile synthesis process of the FLUXNET network (Baldocchi 2008; Agarwal et al. 2008) and other cooperation initiatives, these observations are now available for comparative analysis and generalization. In this publication we present the first synthesis of results from tower CO_2 flux measurements at 118 tower sites representing grassland, cropland, shrubland, savanna and wetland ecosystems of the world-- with the final goal of obtaining measurement-based estimates of their role as net sinks or sources of atmospheric CO_2. Such estimates provide a scientific basis for establishing carbon credit market and poverty alleviation projects.

METHODS

Data for this study were provided by the WorldGrassAgriFlux data set (Gilmanov et al. 2007b) currently including data from 72 nonforest sites (Table 1, method L) for which original 30-min (or 20-min in some sites) net CO_2 flux, F_c, was partitioned into gross

primary productivity, P_g, and ecosystem respiration, R_e, components using light-response function methods (Gilmanov et al. 2003a,b, 2004, 2005, 2006, 2007a). These data were combined with an additional 46 nonforest sites (Table 1, method T) from the FLUXNET La Thuile dataset (Agarwal et al. 2008) that were partitioned into P_g and R_e components using temperature-response methods (Reichstein et al. 2005). In most cases, we used daily P_g and R_e estimates directly from the La Thuile dataset, though sometimes it was necessary to correct negative values of daily gross primary production that were occasionally generated by the night-time temperature response method (cf. Stoy et al. 2006).

In total, tower sites included in our analysis represent 316 site-years of measurements during the 1997-2006 period (Table 1). They are grouped into the following categories: extensively managed grasslands (ungrazed or lightly grazed, uncut or cut occasionally), intensively managed grasslands (regularly cut, grazed, fertilized, irrigated, etc.), croplands, shrublands/savannas, and wetlands. The geographic distribution of sites is illustrated in Fig. 1.

Net Tower Flux (F_c) Partitioning into Photosynthesis (P_g) and Respiration (R_e)

Analysis of flux tower measurements requires processing algorithms (Lee et al. 2004; Burba and Anderson 2007; Baldocchi 2008a) that describe the net result of interacting ecosystem components that absorb CO_2 (mostly, photosynthetic assimilation by autotrophic organisms), and those that release CO_2 (metabolic CO_2 production, R_e, is the major component of CO_2 efflux during the growing season). Because photosynthesis and respiration respond rather differently to major environmental drivers (e.g., Thornley and

Johnson 2000), partitioning of tower-based $\{F_c\}$ data into photosynthetic assimilation and ecosystem respiration components is recognized as an necessary step in post-processing of net flux data for use in predictive modeling of ecosystem carbon cycling (Gilmanov et al. 2003b, 2004, 2005, 2006, 2007a; Reichstein et al. 2005; Stoy et al. 2006).

Using the ecophysiological sign convention (positive flux from atmosphere to ecosystem), and excluding plants with CAM-type metabolism, the instantaneous gross photosynthesis rate, P_g, used in this study was obtained as a sum of daytime net CO_2 exchange, F_c, and daytime ecosystem respiration, R_d, minus the rate of change of CO_2 storage in the atmospheric layer between the soil surface and the CO_2 sensor at the tower (Gilmanov et a. 2007). When estimates of the storage term were not available (e.g. for communities with low canopy height and sufficient turbulent transport) the gross productivity was approximated as:

$$P_g(t) = \begin{cases} F_c(t) + R_d(t), & Q(t) > 0, \\ 0, & Q(t) = 0. \end{cases} \quad [1]$$

where $Q(t)$ is the intensity of photosynthetically active radiation (Gilmanov et al. 2004).

Because direct measurements of the daytime ecosystem respiration R_d are quite difficult to make, two main approaches of its indirect estimation (leading to the two major methods of net flux partitioning into photosynthesis and respiration components) were used:

(i) establishing relationship of the night-time respiration:

$$R_n(t) = \begin{cases} F_c(t), & Q(t) = 0 \\ 0, & Q(t) > 0, \end{cases} \quad [2]$$

to environmental drivers affecting it (e.g., soil temperature, T_s) and using these relationships to estimate daytime respiration, R_d. This approach has been widely used for forest-type ecosystems (Goulden et al. 1996) and was used in this study for the first round of network-level aggregation of the raw 30-min data into daily gross primary productivity and ecosystem respiration values (http://www.fluxdata.org/DataInfo/).

(ii) obtaining estimates of daytime ecosystem respiration R_d through identification of the respiration term in the ecosystem-scale light-response functions describing relationships of the daytime flux F_c to photon flux density, Q, leaf area index, L, soil temperature, T_s, water content of the soil, W_s, air relative humidity, HR, and other factors. In general, light-response functions include rather complicated analytical or algorithmic expressions (e.g., those suggested by Thornley and Johnson [2000, p. 248-249]), taking into account most of the major ecophysiological parameters of photosynthesis (quantum yield α, maximum photosynthesis A_{max}, convexity of the light response, θ, leaf area index, L). When fully expanded, these expressions can require several lines of printed text. At the other end of the complexity spectrum lie simple $F_c(Q)$ relationships like the ramp function by Blackman (1905), Mitscherlich's saturated exponent (1909), and the rectangular hyperbola by Tamiya (1951); the latter being a nearly standard approach to light-response fitting at the early stages of flux tower data

analysis (Ruimy et al. 1995). These simple models are convenient and, in some cases, fit observed data well; however, they share the major drawback of lacking the ability to describe light-response patterns of varying convexity (curvature).

Under the widely accepted eco-physiological framework, the convexity of the light-response is represented by the fraction of diffusion resistance to the total (diffusion + carboxylation) resistance to carbon transport: $\theta = \rho_d/(\rho_d + \rho_x)$ (Thornley and Johnson 2000). Taking into account the differences in leaf morphology and biochemistry in different plant groups (e.g., C_3 vs. C_4 photosynthesis types), the ability to describe light-response curves of different convexity seems to be a necessary requirement for an adequate light-response function model. Our experience with quantification of the tower-based light-response data from a wide range of nonforest ecosystems led us to use the nonrectanglar hyperbolic model (Rabinowich 1951; Thornley and Johnson 2000):

$$F_c(Q; \alpha, A_{max}, \theta, r_d) = \frac{1}{2\theta}\left(\alpha Q + A_{max} - \sqrt{(\alpha Q + A_{max})^2 - 4\alpha A_{max}\theta Q}\right) - r_d, \quad [3]$$

where Q denotes photon flux density, α is the quantum yield, A_{max} maximum gross photosynthesis, θ is the convexity parameter of the light-response curve, and r_d is daytime ecosystem respiration rate, for days when solar radiation is the major driver of daytime CO_2 exchange. This model provides a powerful and flexible tool to describe light-response at the various nonforest tower sites (Gilmanov et al. 2003a,b, 2004, 2005, 2006, 2007a).

Under semi-arid and arid conditions, when significant warming of the soil in the afternoon period is observed, the pattern of data points on the light-response plane {Q,

$F_c\}$ is often characterized by a hysteresis-like loop with the morning branch of the light-response curve lying above the afternoon branch. In such cases, these light-response patterns were effectively described by the modified nonrectangular hyperbolic model (Gilmanov et al. 2003a):

$$F_c(Q, T_s; \alpha, A_{max}, \theta, r_d) = \frac{1}{2\theta}\left(\alpha Q + A_{max} - \sqrt{(\alpha Q + A_{max})^2 - 4\alpha A_{max}\theta Q}\right) - r_0 e^{k_T T_s}, \quad [4]$$

where the daytime respiration term r_d of eq. [3] is modified to $r_0 e^{k_T T_s}$ to represent an exponential increase of respiration with soil temperature, T_s, and k_T and r_0 are empirical parameters estimated in the process of fitting eq. [4] to the daytime data $\{Q(t_i), T_s(t_i), F_c(t_i)\}$, and t_i is time between the sunrise and sunset, $t_r \le t_i \le t_s$. For days described by eq. [4], average daytime respiration rate, r_d, was calculated as:

$$r_d = \frac{r_0}{(t_s - t_r)} \int_{t_r}^{t_s} e^{k_T T_s(t)} dt\,. \quad [5]$$

Numerical fitting of parameters α, A_{max}, θ, r_d or r_0 and k_T of equations [3] or [4] was achieved using procedures from the "Global Optimization Package" by Loehle Enterprises (2009) available under the "Mathematica" software system (Wolfram Research 2009). It should be emphasized that to avoid serious errors of light-response parameter estimation resulting from fitting equations to data lumped over several days (as sometimes can be seen in publications on the subject, e.g., Ruimy et al. 1995; Zhang et al. 2006; Zhao et al. 2006), only single day datasets $\{Q(t_i), T_s(t_i), F_c(t_i)\}$ were used in this

study to identify the light-curves and the light-temperature response surfaces of CO_2 exchange.

It should also be noted that parameters obtained by fitting equations [3] or [4] to flux-tower data sets are ecosystem-scale parameters referring to a ground unit (e.g., per 1 m^2 ground surface) and should be distinguished from leaf-level light-response parameters used in physiological studies, which correspond to units of leaf area (e.g., $A_{L,max}$, α_L, etc.). Only under special conditions (monoculture with convexity $\theta = 0$), is photosynthetic capacity per unit ground area (A_{max}) equal to the product of photosynthetic capacity per unit leaf area ($A_{L,max}$) and the leaf area index (L): $A_{max} = A_{L,max}*L$ (cf. Thornley and Johnson 2000).

For measurement days that allow identification of parameters of models [3] or [4], total daytime respiration, R_d, was calculated as the product of average daytime rate, r_d, and the length of the daylight period:

$$R_d = r_d(t_s - t_r). \qquad [6]$$

For days with daytime data inappropriate for light-response analysis, parameters k_T and r_0 were estimated by fitting an exponential equation $F_c = r_0 e^{k_T T_s}$ to the nighttime data $\{T_s(t_i), F_c(t_i)\}_{Q(t_i)=0}$.

Eventually, total daily gross primary production, P_g, was obtained as the sum of daytime respiration total R_d and the daytime net flux integral, $P_d = \int_{t_r}^{t_s} F_c(t)dt$:

$$P_g = P_d + R_d. \quad [7]$$

Gap-filling of P_g and R_e values for days with missing measurements was achieved using various methods characterized in the recent review by Moffat et al. (2007), with particular emphasis on (i) extrapolation of parameters of light- and temperature-response functions to days with missing flux measurements, calculations of fluxes at the 30-min time scale, and estimation of daily P_g and R_e values as integrals of corresponding 30-min estimates; and (ii) nonlinear regressions of daily P_g and R_e values from daily aggregated values of predictors such as photosynthetically active radiation, air and soil temperature, soil water content, etc.

Seasonal Patterns of Parameter Dynamics

Numerical estimation of the major light-response parameters on a daily basis, i.e. obtaining the values α, A_{max}, θ, r_d for as many days t as allowed by the quality and quantity of the data, permits evaluation of time-functions $\alpha(t)$, $A_{max}(t)$, $\theta(t)$, $r_d(t)$ characterizing seasonal patterns of the dynamics of these parameters. These patterns are revealed most clearly through smoothing of the empirical time series of the parameter estimates. In this study we used one of the simplest and easily interpretable methods – calculation of the mean parameter value and its standard error, e.g., $\left\{\overline{\alpha}_j, s_{\overline{\alpha}_j}\right\}$, $\left\{\overline{A}_{\max,j}, s_{\overline{A}_{\max,j}}\right\}$, etc. for every calendar week, j, of the year of observations (j = 1, …, 52}. Using weekly average values instead of individual daily estimates proved to be most appropriate for comparison between ecosystems and years,

particularly for such parameters as quantum yield, α, exhibiting large day-to-day variability.

Seasonal Dynamics and Annual Budgets of GPP, RE, and NEE

Estimated values of $P_g(t)$ and $R_e(t)$ for the year-round or observation period were integrated over the 365 days (or over the measurement season – when no year-round data were available) to obtain annual (seasonal) totals of gross primary production, *GPP*, and total ecosystem respiration, *RE*. Cumulative *NEE* total to day *t*, *CumNEE(t)*, was calculated by integrating daily values of $F_c(t) = P_g(t)-R_e(t)$. The net ecosystem CO_2 exchange for years or growing seasons, *NEE*, was calculated as the difference (*GPP–RE*).

Ecosystem-Scale Light-Use Efficiency

Comparative physiological studies at the leaf, individual, or population level commonly calculate the light-use efficiency of gross photosynthesis P_g with respect to absorbed photosynthetically active radiation, Q_a, resulting in a *gross physiological* light-use efficiency coefficient (Larcher 1995):

$$\varepsilon_{phys} = \frac{P_g}{Q_a}, \qquad [8]$$

where both the photosynthesis P_g and absorbed radiation Q_a are expressed in molar units (e.g., it is convenient to measure ε in mmol CO_2 per mol quanta). However, in comparative ecological studies it is preferable to use the coefficient of *gross ecological*

light-use efficiency (cf. Odum 1959 (p. 54); Cooper 1970; Austin et al. 1978; Colinvaux 1993):

$$\varepsilon_{ecol} = \frac{P_g}{Q}, \qquad [9]$$

calculated per unit of *total incoming* photosynthetically active radiation, Q. It should be emphasized that while the physiological light-use efficiency coefficient, ε_{phys}, characterizes physiological and biochemical parameters (and is often used in studies performed at the unit leaf area or unit of photosynthetically active biomass basis), ε_{ecol}, as a rule, is calculated per unit ground surface (m^{-2}, ha^{-1}, etc.), and thus also takes into account such ecosystem-level properties as population density, aboveground biomass, and leaf area. Thus, gross ecological light-use efficiency characterizes ecosystems as a whole with respect to ability for utilization of available radiation resources. For example, consider two ecosystems with physiologically similar species and therefore similar light-use efficiencies per unit leaf area, but with LAI in the first ecosystem twice as small as the second (e.g. due to management). For moderate LAI values (e.g., < 3 m^2m^{-2} in the second ecosystem), the photosynthetic uptake per unit of ground surface, P_g, and the absorbed radiation, Q_a, in the second ecosystem will be approximately twice as large as in the first, so that there will be little difference between the two ecosystems in terms of their physiological light-use efficiency ε_{phys}. On the other hand, the incoming radiation, Q, will be the same in the two ecosystems, resulting in ecological light-use efficiency, ε_{ecol}, in the second ecosystem being two times higher than in the first.

RESULTS AND DISCUSSION

Light-Response Functions and Parameters

Within the broad range of climatic conditions and ecosystem types represented in the data set, we observed a variety of patterns of light-response. For comparative purposes, it is convenient to distinguish four major categories differentiated in terms of convexity and presence of the hysteresis-like loop on the light-response scatter diagram $\{Q, F_c\}$ (Fig. 2). In the latter case, plotting the 3-D scatter diagram of the diurnal dynamics of the measurement data and of the response surface $F_c(Q, T_s)$ (eq. [4]) fitted to them provides a partial explanation the loop on the 2-D $\{Q, F_c\}$ plot caused by the increase of ecosystem respiration with the increase of temperature in the afternoon hours (Fig. 3). For the cases shown in Figures 2 and 3, numerical estimates and statistical characteristics of parameters in equations [3] and [4] are presented in Tables 2 and 3.

Nonrectangular hyperbolic equation [3] and its modification [4] taking into account temperature-dependence of daytime respiration, were found to be good numerical tools to fitting light-responses of nonforest ecosystems for days when photosynthetically active radiation was the dominant factor governing the ecosystem CO_2 exchange. It is important to emphasize that the nonrectangular hyperbola provided a close fit to light-response data and provided consistent estimates of the light-response parameters for days when the $\{Q,F_c\}$ plots showed no saturation with respect to Q and were characterized by convexity parameter θ close to 1 (cf. Fig. 2A). The rectangular hyperbola, Mitscherlich's equation, and other approximations lacking convexity parameter fitted to data with such a pattern, yield highly biased estimates of the initial slope, plateau, and the intercept parameters.

Estimates of the apparent quantum efficiency, α, in nonforest ecosystems cover a wide range of values (Fig. 4A), from 5 mmol mol^{-1} in the desert shrublands of Central Asia (Karrykul) to 75 mmol mol^{-1} in intensively managed grasslands of the North Atlantic (Cabauw, the Netherlands), with mean value α_{nonfor} = 33.3 mmol mol^{-1} and standard deviation s_{nonfor} = 14.2 mmol mol^{-1}. The lower 10% quantile of the α values in the sample (5-17 mmol mol^{-1}) included extensively managed arid and semiarid grasslands and shrublands (Karrykul, Cottonwood, Karnap, Audubon, Lethbridge, Kherlenbayan, Tojal, and Fort Peck), while the upper 10% quantile (50-75 mmol mol^{-1}) encompassed intensively managed grasslands (Cabauw, Carlow, Neustift, Easter Bush, Oensingen, Lille Valby, Grillenburg, Haller, Rigi-Seebodenalp), extensively managed grasslands under favorable weather conditions (Laqueuille-extensive, Jornada), and intensive agricultural crops (Lonzee). Interestingly, most productive crop sites, characterized by the highest A_{max} and $P_{g,max}$ values, did not make it to the upper 10% quantum yield quantile, though they belong to the upper 20% quantum yield quantile.

In addition to scatter plots for the pooled data set, understanding relationships between parameters within a particular ecosystem is of interest. Presently, only a subset of extensively managed grasslands shows scatter diagrams with pronounced patterns of co-variation (Fig. 5).

In evaluating obtained estimates of the quantum yield, we should first note that our maximum estimate of 75 mmol mol^{-1} is only two thirds of the theoretical maximum of quantum efficiency of gross photosynthesis estimated by Good and Bell (1980) as 110 mmol mol^{-1}. Comparing our nonforest estimates with those reviewed by Ruimy et al. (1995), from which we estimated mean $\overline{\alpha}_{forest}$ = 37 mmol mol^{-1} with standard

deviation s_{forest} = 17 mmol mol^{-1} (we have excluded data in Ruimy et al. 1995 with α values greater than theoretical maximum of quantum efficiency), one can see that quantum efficiency of nonforest ecosystems is not statistically different from forests. In fact, $\alpha_{max,nonforest}$ estimated for intensively managed Cabauw grassland in The Netherlands (75 mmol mol^{-1}) was numerically higher, but statistically not significantly different from the maximum quantum efficiency determined for the chestnut coppice near Paris, France ($\alpha_{max,forest}$ = 73 mmol mol^{-1}) (Mordacq et al 1991).

The values of maximum average weekly gross photosynthesis, A_{max}, for nonforest sites of the world (Fig. 4A) span from 0.2 mg CO_2 m^{-2} s^{-1} (Fort Peck mixed prairie during a drought year) to 3.4 mg CO_2 m^{-2} s^{-1} (Mead, irrigated continuous corn), with the lower 10% quantile (0.2-0.36 mg CO_2 m^{-2} s^{-1}) including Fort Peck, Dubois, Miles City, Kherlenbayan, Xilinhot, Karrykul, Kubuqi, Burns, and Karnap, and the upper 10% quantile (2-3.4 mg CO_2 m^{-2} s^{-1}) including intensive crops (Mead, Bondville, Lonzee, Ames), intensively managed grasslands (Cabauw, Carlow, Lille Valby), and tallgrass prairies (Shidler, Fort Reno). The mean photosynthetic capacity of nonforest ecosystems, 1.2 mg CO_2 m^{-2} s^{-1} (SD = 0.68 mg CO_2 m^{-2} s^{-1}), lies at the upper end of the mean A_{max} range for different forest types from eddy covariance estimates, 0.66 mg CO_2 m^{-2} s^{-1} to 1.3 mg CO_2 m^{-2} s^{-1} (mean = 0.97 mg CO_2 m^{-2} s^{-1}) (Falge et al. 2002; Funk and Lerdau 2004). At the same time, the highest A_{max} value for nonforest ecosystems found in intensive corn cultures of the Midwest of the USA (3.4 mg CO_2 m^{-2} s^{-1}) were substantially higher than A_{max} = 2.64 mg CO_2 m^{-2} s^{-1} estimated from data by Jarvis (1994) for a Sitka spruce culture in Scotland.

The values of daytime ecosystem respiration rate, r_d, in all ecosystems remained substantially lower than corresponding A_{max} values (cf. Fig. 6, left), but also displayed substantial variability among ecosystem types (Fig. 4B), with maximum weekly average r_d ranging from 0.04 mg CO_2 m^{-2} s^{-1} (Burns, drought year) to 0.50 mg CO_2 m^{-2} s^{-1} (Haller, warm and wet year). The lower 10% quantile of maximum weekly r_d values included arid and semiarid grasslands and shrublands (Burns, Karnap, Kherlenbayan, Karrykul, Cottonwood, Burns, Dubois, Kubuqi) and tundra (Barrow), while the upper 10% quantile of r_d distribution was represented by intensively managed grasslands (Haller, Neustift, Cabauw, Carlow, Oensingen, Lille Valby, Easter Bush), intensive crops (Ames, Mead), tallgrass prairies (Shidler, Rannels Ranch), and a semidesert grassland in a year with exceptionally high precipitation (Jornada).

The weekly maxima of the coefficient of gross ecological light-use efficiency, ε, resulting from this study were in the range from 3 to 59 mmol mol^{-1} (mean 22, standard deviation 12.4 mmol mol^{-1}), and, understandably, were lower than the weekly maxima of the apparent quantum yield, α (Fig. 6, right). It is interesting, however, that for some ecosystems, particularly for agricultural C_4-crops and tropical grasslands dominated by C_4-species, ε values were not considerably lower than α (e.g., see Fig. 6E, 6F and 6H, right). This is a direct result of relatively high values of the convexity coefficient of the light-response curves of C_4 species; at the ultimate case of $\theta = 1$, the values of α and ε will become equal, provided input radiation levels remains within the range of linear light-response.

On the contrary, in C_3-communities characterized by lower convexity values ($\theta =$ 0 in the extreme case of rectangular hyperbolic light-response), ecological light-use

efficiency remains substantially lower than quantum yield (Fig. 6A, right). The lower 10% quantile of light-use efficiency values ε (2.6 – 6.4 mmol mol^{-1}) includes deserts, desert and dry steppe grasslands, shortgrass and sagebrush steppes, mixed prairies, California grasslands and chaparral, and tundra (Karrykul, Karnap, Audubon Ranch, Kendall, Xilinhot, CPER, Fort Peck, Cottonwood, Burns, Kubuqi, Kherlenbayan, Sky Oaks, Barrow, Atqasuk, Ivotuk). The upper 10% quantile of the ε values (40-59 mmol mol^{-1}) mostly includes high-yield crops (Risbyholm, Langerak, Molenweg, Mead, Bondville, Oensingen, Gebesee, Lonzee, Batavia), as well as highly productive intensively and extensively managed grasslands (Carlow, Lille Valby, Oensingen, Neustift).

For comparison with ε_{max} estimates for nonforest ecosystems, we calculated average weekly values of light-use efficiency for the twelve most productive forest ecosystems in the FLUXNET La Thuile database. These twelve ε_{max} values ranged between 29.1 and 47.7 mmol mol^{-1}, with the highest value corresponding to the 2001 data set for the Duke loblolly pine forest (North Carolina), which is less than ε_{max} = 59 mmol mol^{-1} for a high-yield crop (also, see Table 5 for $P_{g,max}$ comparison of forests and nonforest ecosystems). Thus, the light-use efficiency data are in agreement with observations earlier in this section that the values of the maximum apparent quantum yield in nonforest ecosystems (particularly, intensively managed grasslands) are comparable and even higher than those for forest ecosystems.

Parameter Interrelations

As expected, numerical values of light-response parameters among different ecosystems did not vary independently of each other, but demonstrated patterns of correlation shown in Figs. 4 and 5. Our results for this extensive data set are in agreement with earlier studies based on smaller subsets of flux-tower data, suggesting that the plateau parameter of gross photosynthesis, A_{max}, is a good predictor for other light-response parameters, including quantum yield, α, ecosystem respiration rate, r_d, and light-use efficiency, ε (Gilmanov et al. 2007a; Owen at al. 2007). Baldocchi and Xu (2005) found that A_{max} is a good predictor for another photosynthetic parameter, the maximum rate of carboxylation, $V_{c,max}$. Nevertheless, while in previous studies mostly linear relationships between A_{max} and other parameters were identified, the wider range of parameter variations in our data set has revealed a number of distinct nonlinearities. For example, an allometric relationship $\alpha = 30.36(A_{max})^{0.55}$ with R^2 value of 0.55 was obtained for the relationship between apparent quantum yield and maximum photosynthesis (Fig. 4A). The better fit of the allometric (nonlinear) description of the $\alpha(A_{max})$ relationship compared with the simple linear model is demonstrated by the fact that the nonlinear model conveys a decrease in α with decreasing A_{max} as the latter is approaching zero, while the linear model predicts an unrealistic α_0 value of ~15 mmol mol^{-1} even when A_{max} $\rightarrow 0$.

Daytime ecosystem respiration, r_d, also demonstrated an allometric relationship to A_{max} described as $r_d = 0.22(A_{max})^{0.71}$ characterized by $R^2 = 0.69$ (Fig. 5B). In this case, the linear model also provided a reasonable fit to the data ($R^2 = 0.67$), though its applicability to areas with low A_{max} values is limited by an unrealistically high intercept of $r_{d0} = 0.09$ mg CO_2 m^{-2} s^{-1} as $A_{max} \rightarrow 0$. From the patterns of data points on Figs. 5C

and 5D one may see that the relationships between ecological light-use efficiency, maximum daily gross photosynthesis, and L_{max} may be approximated by both the linear, and the allometric equations, though the latter provides better description in the lower range of A_{max} and L_{max}.

For various reasons, not all flux sites collected data on maximum leaf area (L_{max}) and/or maximum aboveground green biomass (G_{max}). Nevertheless, with the limited data available (Figs. 5F and 5H) we were able to establish nonlinear allometric (with allometry coefficient < 1) dependence of maximum photosyntyhesis parameters (A_{max}, $P_{g,max}$) and the standard morphometric characteristics such as maximum aboveground biomass, G_{max} and maximum leaf area index, L_{max} (Figures. 5F and 5H).

Seasonal Patterns of Parameter Dynamics

Because light-response parameters evaluated from flux-tower measurement data sets represent not only physiological characteristics (which also change in time with phenology and environmental conditions) but also the ecosystem-scale attributes like aboveground biomass, leaf area index and others, such parameters exhibit pronounced variation in magnitude during the year. Seasonal changes of these parameters, though specific for particular sites and years, have general patterns that are revealed by time-plots of parameter values aggregated at the weekly time step (Fig. 6). Pronounced seasonal dynamics of light-response parameters shown on Fig. 6 in cold and temperate environments is apparently driven by radiation and temperature inputs (Fig. 6, A, D), while under arid conditions it mainly reflects fluctuation of precipitation (Fig. 6 E, F). This climatically driven unimodal pattern of seasonal parameter change was particularly

pronounced in species-poor ecosystems or monocultures with relatively narrow production period, be that a floodplain meadow in the tundra zone (Fig. 6A) or agricultural crops (Figs. 6G and 6H). In ecosystems with higher species diversity and broader production period (up to year-round production in tropical conditions), the general seasonal pattern of parameter dynamics was compounded by additional fluctuations reflecting different reactions of various species groups (e.g., cool and warm-season grasses) to weather variability and management pressure (grazing, mowing) during various parts of the year (Figs. 6 B, C, D). These data may help to explain difficulties experienced by those attempting to simulate year-round dynamics of gross primary productivity and light-response parameters by modification of the hypothetical maximum parameter value by factors-multipliers describing effects of various drivers like radiation, temperature, moisture, etc. (cf. Monteith 1972; Ciais et al. 2001).

Seasonal Dynamics and Annual Budgets of GPP, RE, and NEE

Depending on a number of external (e.g. radiation, temperature, precipitation) and internal ecological factors (e.g. leaf area, phenological state, water and nutrient supply), the functions of gross primary productivity, $P_g(t)$, and total ecosystem respiration, $R_e(t)$, demonstrated pronounced temporal dynamics during the year, as exemplified by the measurement-based estimates of $P_g(t)$ and $R_e(t)$ presented on Fig. 7. On the other hand, the curve of cumulative net ecosystem exchange, $CumNEE(t)$ showed much smoother behavior, and its value at the end of the year, NEE, provides a summary of ecosystem carbon budget.

Data from the WorldGrassAgriFlux data set demonstrated a great variety of seasonal patterns of productivity and respiration dynamics, some of the typical curves are illustrated in Fig. 7. There are three major seasonal patterns of the cumulative NEE curve: (i) equilibrium (S-shaped), (ii) permanent accumulation, and (iii) permanent release of carbon. The equilibrium pattern (i) characterizing non-harvested ecosystems with marked seasonality of primary productivity was exemplified by data from a floodplain tundra meadow at Cherskii in the Far North-East of Russia (Fig. 7A). With the period of decomposition activity (May-September) completely encompassing the production period (June-August) and with maximum decomposition lagging behind maximum production, the curve of cumulative *NEE* assumed a characteristic S-shaped form with the net annual ecosystem CO_2 exchange nearly zero. The accumulative pattern (ii) is described by the more or less monotonous accumulation of net ecosystem production in ecosystems with a period of marked domination of production over decomposition processes observed in both grassland (Fig. 7F) and cropland ecosystems (Fig. 7G). The third pattern (iii) – nearly permanent domination of respiratory efflux over assimilatory uptake resulting in significant net loss of carbon from the ecosystem at the end of the year, as exemplified by measurements at the Audubon (AZ) desert grassland on a high carbonate soil (Emmerich 2003) (Fig. 7D). These three major patterns were accompanied by a variety of intermediate variants with local maxima and minima of the *CumNEE(t)* curve reflecting weather fluctuations and harvesting, finally leading to either net uptake (Fig. 7C) or net loss of carbon from the ecosystem (Fig. 7B, 7E and 7H).

Year-round integration of the $P_g(t)$, $R_e(t)$, and $F_c(t)$ curves provided estimates of annual *GPP*, *RE*, and *NEE* totals for all the site-years in this study. These data stratified

by major ecosystem groups (extensively and intensively managed grasslands, shrublands and savanna, wetlands, and croplands) are summarized in Table 4. The highest mean gross primary production (5767 g CO_2 m^{-2} yr^{-1}) and ecosystem respiration (4990 g CO_2 m^{-2} yr^{-1}) were achieved in intensively managed grasslands. Not surprisingly, the highest mean annual net ecosystem CO_2 exchange (933 g CO_2 m^{-2} yr^{-1}) was found in croplands. To supplement these basic statistical characteristics, Fig. 8 shows the distributions of the *GPP, RE*, and *NEE* values in the pooled data set of estimates from all site-years in the database. They show that while the *GPP* and *RE* values in our sample had a wide range of variation (95 - 8600 g CO_2 m^{-2} yr^{-1} for gross production and 112 - 7880 g CO_2 m^{-2} yr^{-1} for respiration), with *GPP* and *RE* values fairly well distributed over their ranges (Fig. 8A and 8B), the net CO_2 exchange values concentrated between -1342 g CO_2 m^{-2} yr^{-1} and 2394 g CO_2 m^{-2} yr^{-1} had a distinctly unimodal distribution (Fig. 8 C). The average *NEE* value for our sample of 316 nonforest ecosystems is 485 g CO_2 m^{-2} yr^{-1} (SD = 696 g CO_2 m^{-2} yr^{-1}). Comparing these statistics with the mean (671 g CO_2 m^{-2} yr^{-1}) and standard deviation (988 g CO_2 m^{-2} yr^{-1}) of published *NEE* values for 506 site-years from flux towers worldwide (Baldocchi 2008b), we did not detect a difference between the two *NEE* averages at the 1% level of significance. The higher mean *NEE* value for Baldocchi's sample is easily explained, taking into account that it contains a number of growing forest sites with high *NEE*, while the WorldGrassAgriFlux data set includes mostly nonforest sites (with occasional near-climax shrubland and savanna ecosystems). A particularly interesting question, in the context of comparing basic parameters of the carbon cycle, regards identifying maximum rates of photosynthetic CO_2 assimilation in various ecosystems. For this purpose, in Table 5 we have compiled the data of the two

dozen (or maximum available) site-years with maximum values of daily photosynthesis, $P_{g,max}$, and annual *GPP* for our five types of nonforest ecosystems and for the forest sites represented in the most recent FLUXNET database. With respect to the annual *GPP,* forest ecosystems achieved the highest estimates of photosynthetic CO_2 uptake, with maximum *GPP* = 14339 g CO_2 m^{-2} yr^{-1} for a tropical forest in French Guyana (Table 5F) compared to maximum *GPP* = 8600 g CO_2 m^{-2} yr^{-1} for a tropical grassland in Rondonia, Brazil (Table 5 A). In contrast, maximum daily rates of photosynthetic uptake were recorded not in forests, but in the intensive crops of the Midwestern United States, with $P_{g,max}$ = 116 g CO_2 m^{-2} d^{-1} estimated for irrigated corn in a corn-soybean rotation (Mead, NE) in 2001 (Table 5E). These data clearly demonstrate that even in other types of nonforest ecosystems (e.g. shrublands and savanna), in addition to intensive agricultural crops, maximum rates of gross photosynthetic assimilation (50 – 76 g CO_2 m^{-2} d^{-1}) are quite comparable to those in most productive forests (55 – 99 g CO_2 m^{-2} d^{-1}). Apparently, the major reason why annual *GPP* in forests is typically higher than nonforested ecosystems is the length of production period. In tropical forests, production may encompass the whole year, while in most nonforest ecosystems it is temporally limited by temperature and water availability.

Source/Sink Activity of Nonforest Ecosystems

The data on annual budgets of production, respiration, and net exchange of nonforest ecosystems obtained in our study allow quantitative consideration of important question about the magnitude and significance of the source or sink activity of various ecosystem types. Since H.T. Odum (1956) (see also Baldocchi 2008b), a convenient way to visualize the net carbon budget of ecosystems for comparative purposes is to construct an

RE versus GPP scatter diagram and compare the distribution of data points with respect to the 1:1 diagonal. Points below the diagonal correspond to sinks (*GPP* > *RE*, *NEE* >0), while points above the diagonal describe sources of carbon (*GPP* < *RE*, *NEE* < 0). H.T. Odum's plot for the whole nonforest data set (Fig. 9) demonstrates that for four out of every five site-years, gross production was higher than ecosystem respiration, indicating net ecosystem sink activity. Stratification of the data with respect to ecosystem type (Fig. 10) shows that for all types of nonforest ecosystem in our database there were considerably more years with net CO_2 uptake than release. However, years with net source activity occasionally occurred in all ecosystems except wetlands.

The distributions of *NEE* for different ecosystems presented in Fig. 11 provide a more detailed description of the matter. Source-type activity more frequently occurred in extensively managed grasslands, shrublands/savanna, and croplands, than in intensively managed grasslands and wetlands. As a rule, source-type activity was associated with years of drought, excessive grazing and hay mowing, high organic matter content of soils (e.g. grasslands on peat) or high $CaCO_3$ reserves in the soil profile, and transitional successional status of the ecosystem (e.g., grasslands of previously forested soils). For agroecosystems, source activity is often observed in crops with intensive soil preparation and relatively short leaf duration periods (e.g. soybeans). However, it should be emphasized that for all ecosystems examined in our study, carbon sink activity was frequently observed, with the highest net carbon uptakes in intensively managed grasslands and cropland ecosystems (Fig. 11, Table 4).

These observations are in obvious contradiction with conclusion of the first State Of the Carbon Cycle Report (SOCCR) (King et al. 2007) and some earlier authors (e.g.,

Reicosky 1997; Smith and Falloon 2005) who emphasized net source or neutral activity of agricultural ecosystems. In this context, it is appropriate to consider the argument by C. Körner (2003) regarding the critical significance of the representativeness of flux tower data sets. Recognizing the relevance of Körner's arguments to the situation in the early 2000s, it should be emphasized that, at least with regard to nonforested ecosystems, the present set of flux tower sites includes a wide range of climatic conditions and management regimes and, therefore, is much less biased towards highly productive ecosystems.

Ecosystem-Scale Production and Respiration in Relation to Major Ecological Factors

Relationships of production and decomposition to major ecological factors attracted attention of ecologists and geographers of the 20th century (Weaver 1924; Walter 1939; Budyko and Efimova 1968; Rosenzweig 1968; Lieth 1975) and were later approached under the framework of dynamic global vegetation models (DGVM) and related models (e.g., Woodward et al. 2001; Cramer et al. 2001). Presently, these problems are back in the focus of ecosystem, regional and global ecology, not only because of the recognition of their relevance to global climatic change, but also because today, for the first time, measurement-based quantitative estimates of gross productivity and total ecosystem respiration are readily available through post-processing of net CO_2 exchange measurements at flux towers.

Besides radiation and temperature, which are already taken into account by the light-temperature-response function method, the next most important factor influencing ecosystem productivity and respiration is water (e.g., Slatyer 1967; Boyer 1982). Though

water content or water potential of top-soil horizons are the most desirable predictors for production and decomposition modeling, such data are not yet readily available for many flux tower stations, making it necessary for us to limit consideration to available precipitation data.

Both theory and empirical data indicate nonlinear relationships between photosynthesis, productivity, and decomposition rates on water content and/or water potential (Denmead and Shaw 1962; Wildung et al. 1975; Singh et al. 1980; Eastin and Sullivan 1984; Mielnick and Dugas 2000). In contrast, observations of the linear response of productivity in certain ecosystem types occasionally appear in the literature (Walter 1939; Le Houèrou and Hoste. 1977; Sala et al. 1988). Our data allow a fresh look at this old problem using new ecosystem-scale estimates of *GPP* and *RE* values in relation to precipitation *PCPN* (Fig. 12-14). Within the whole WorldGrassAgriFlux data set, we found that the subsets of extensively managed grasslands, intensively managed grasslands, and shrublands-savanna exhibit patterns of relationship of *GPP* and *RE* to precipitation and dryness index, while the data for wetlands and croplands did not produce recognizable patterns.

Gross production and ecosystem respiration of extensively managed grasslands demonstrate nonlinear patterns in response to annual precipitation that may be expressed by Mitscherlich's equation (Fig. 12A and 12B) describing a saturated relationship (cf. Lieth 1975). Deviation of the data points from the trend, which increases in amplitude with increasing precipitation, indicates a diminishing response to precipitation. As shown in Figs. 12C and 12D, the decrease of precipitation use efficiency is linked to the dryness index (ratio of annual net radiation, R_{net}, to the amount of energy required for evaporation

of precipitation, λ*PCPN*, where λ is the latent heat coefficient) (Budyko and Efimova, 1968; Long et al. 1991).

Intensively managed grasslands, which are typically located in climates with more favorable precipitation and less drought stress, still exhibit responses to precipitation and dryness; this response is especially pronounced for gross primary production (Fig. 13). Shrublands and savanna ecosystems, with their broad range of precipitation and dryness index, demonstrate strong nonlinearity of response to precipitation and dryness for both the assimilation and respiration components of the carbon cycle (Fig. 14).

CONCLUSIONS AND IMPLICATIONS

The light-response parameters of nonforest terrestrial ecosystems have a wide range of variability, from relatively low values of photosynthetic capacity (A_{max} = 0.2 mg CO_2 m^{-2} s^{-1} in drought-stressed grasslands), quantum yield (α = 5 mmol mol^{-1} in deserts), daytime ecosystem respiration (r_d = 0.04 mg CO_2 m^{-2} s^{-1} in drought-stressed sagebrush steppe), and gross ecological light-use efficiency (ε = 2.6 mmol mol^{-1} in sedge and tussock tundras of Alaska), to the highest values ever recorded for terrestrial ecosystems (intensively managed grasslands and agricultural crops: A_{max} = 3.4 mg CO_2 m^{-2} s^{-1}, α = 75 mmol mol^{-1}, r_d = 0.50 mg CO_2 m^{-2} s^{-1}, ε = 59 mmol mol^{-1}). Under optimal conditions, gross primary productivity in nonforest terrestrial ecosystems can surpass productivity of forests, with maximum rates of daily gross photosynthetic assimilation, $P_{g,max}$, achieving values greater 100 g CO_2 m^{-2} d^{-1} in intensive agricultural crops ($P_{g,max}$ = 116 g CO_2 m^{-2} d^{-1}), while for forest ecosystems $P_{g,max}$ values remain below 100 g CO_2 m^{-2} d^{-1} (FLUXNET data base: www.fluxdata.org). Nevertheless, due to limitation by radiation, temperature, water, and nutrient resources, as well as management practices, maximum values of annual gross photosynthesis (*GPP*) of nonforest ecosystems estimated from flux-tower measurements remain below 10000 g CO_2 m^{-2} yr^{-1}, while in many types of forests they considerably exceeded this value (with maximum *GPP* > 14000 calculated for a tropical forest in French Guyana). The annual values of both *GPP* and *RE* for extensively and intensively managed grasslands, and shrubland/savanna ecosystems are nonlinearly related to annual precipitation, *PCPN*, and dryness index, $R_{net}/(\lambda*PCPN)$, indicating the potential sensitivity of these ecosystems to anthropogenic climate change.

The average annual net CO_2 exchange of our sample of 316 *NEE* values for nonforest ecosystems indicates that on average, nonforest ecosystems act as net sinks for atmospheric CO_2, with the highest rates of annual CO_2 uptake in agricultural crops (mean NEE_{crop} = 933 g CO_2 m^{-2} yr^{-1}) and intensively managed grasslands (mean $NEE_{grassint}$ = 848 g CO_2 m^{-2} yr^{-1}). These data, based on continuous long-term flux-tower measurements, confirm that grasslands and agricultural crops play a significant role in the carbon budget and have high carbon sequestration potential (Lal et al. 1998; Follett et al. 2001; Follett and Schuman 2005). These findings directly contradict conclusions of earlier authors (e.g., Smith and Faloon 2005; Conant et al. 2007 in SOCCR) about the negative or nearly neutral role agroecosystems play in continental carbon budgets. These earlier studies were based on C-inventory methods and did not utilize flux-tower measurements. Clearly, further analyses are needed to determine the extent to which flux-tower networks and the GIS and remote-sensing methods used to up-scale flux measurements to the regional level are representative, and to support our conclusion about the significant sink role of managed grasslands and intensive agricultural crops in the carbon budget.

ACKNOWLEDGEMENTS

The authors thank managers of the RANGEFLUX data base Patricia Mielnick and the FLUXNET data base Dario Papale, Markus Reichstein, and Deb Agrawal for assistance with updating tower flux data. We also thank Mary Brooke McEachern for help with editing the manuscript of the paper.

LITERATURE CITED

Agarwal, D., M. Humphrey, C. van Ingen, N. Beekwilder, M. Goode, K. Jackson, M. R. L. Rodriguez, and R. Weber. 2008. FLUXNET snthesis dataset collaboration infrastructure. *FluxLetter (The Newsletter of FLUXNET)* 1: 5-7.

Austin, R. B., G. Kingston, P. C. Longden, and P. A. Donovan. 1978. Gross energy yields and the support energy requirements for the production of sugar from beet and cane: a study of four production areas. *Journal of Agricultural Science* 91:661-675.

Baldocchi, D. 2008a. *Advanced topics in biometeorology and micrometeorology. http://nature.berkeley.edu/biometlab/espm228/.*

Baldocchi, D. 2008b. "Breathing" of the terrestrial biosphere: lessons learned from a global network of carbon dioxide flux measurement systems. *Australian Journal of Botany* 56: 1-26.

Baldocchi, D., and L. Xu. 2005. Carbon exchange of deciduous broadleaved forests in temperate and Mediterranean regions. *In:* H. Griffiths and P. G. Jarvis, editors. The carbon balance of forests. Taylor and Francis, New York, p. 187-215.

Birdsey, R. A., J. C. Jenkins, M. Johnston, E. Huber-Sannwald, B. Amero, B. de Jong, J. D. E. Barra, N. R. French, F. Garcia-Oliva, M. Harmon, L. S. Heath, V. J. Jaramillo, K. Johnsen, B. E. Law, E. Martin-Spiotta, O. Masera, R. Neilson, Y. Pan, and K. S. Pregitzer. 2007. North American Forests. in A. W. King, L. Dilling, G. P. Zimmerman, D. M. Fairman, H. R.A., G. Marland, R. A.Z., and T. J. Wilbanks [eds.]. The First State of the Carbon Cycle Report (SOCCR): The North American Carbon Budget and Implications for the Global Carbon Cycle. A Report by the U.S. Climate Change Science

Program and the Subcommittee on Global Change Research. National Oceanic and Atmospheric Administration, National Climatic Data Center, Asheville, NC, USA, p. 117-126.

Blackman, F. F. 1905. Optima and limiting factors. *Annals of Botany* 19: 281-295.

Boyer, J.S. 1982. Plant productivity and environment. *Science* 218:443-448.

Bridgham, S. D., J. P. Megonigal, J. K. Keller, N. B. Bliss, and C. Trettin. 2007. Wetlands. *In*: A. W. King, L. Dilling, G. P. Zimmerman, D. M. Fairman, H. R.A., G. Marland, R. A.Z., and T. J. Wilbanks [eds.]. The First Stata of the Carbon Cycle Report (SOCCR): The North American Carbon Budget and Implications for the Global Carbon Cycle. A Report by the U.S. Climate Change Science Program and the Subcommittee on Global Change Research. National Oceanic and Atmospheric Administration, National Climatic Data Center, Asheville, NC, USA, p. 139-148.

Budyko, M. I., and N. A. Efimova. 1968. The use of solar energy by the natural plant cover of the USSR. *Botanicheskii Zhurnal* 53:1384-1389.

Burba, G., and D. Anderson. 2007. *Introduction to lthe eddy covariance method. General guidelines, and conventional workflow. LI-COR Biosciences. http://www.licor.com/env/PDF_Files/EddyCovariance_readonly.pdf.*

Buyanovsky, G. A., and G. H. Wagner. 1998. Changing role of cultivated land in the global carbon cycle. *Biology and Fertility of Soils* 27:242-245.

Ciais, P., P. Friedlingstein, A. Friend, and D. S. Schimel. 2001. Integrating global models of terrestrial primary produuctivity. In: J. Roy, B. Saugier, and H. A. Mooney [eds.] Terrestrial global productivity. Academic Press, San Diego et al., p. 449-478.

Colinvaux, P. A. 1993. Ecology 2. Wiley, New York.

Conant, R. T., K. Paustian, F. Garcia-Oliva, H. H. Janzen, M. J. Jaramillo, D. E. Johnson, and S. N. Kulshreshtha. 2007. Agricultural and grazing lands. *In:* A. W. King, L. Dilling, G. P. Zimmerman, D. M. Fairman, R. A. Houghton, G. Marland, A. Z. Rose, and T. J. Wilbanks, editors. The first state of the carbon cycle report (SOCCR): The North American carbon budget and implications for the global carbon cycle. A report by the U.S. Climate Change Science Program and the Subcommittee on Global Change Research. National Oceanic and Atmospheric Administration, National Climatic Data Center, Asheville, NC, USA, p. 107-116.

Cooper, J. P. 1970. Potential production and energy conversion in temperate and tropical grasses. *Herbage Abstracts* 40:1-13.

Cramer, W., R. J. Olson, S. D. Prince, J. M. O. Scurlock, and members_of_the_Global_Primary_Production_Data_Initiative. 2001. Determining present patterns of global productivity. *In:* J. Roy, B. Saugier, and H. A. Mooney [eds.]. Terrestrial global productivity. Academic Press, San Diego et al., p. 429-448.

Davidson, E. A., and I. A. Janssens. 2006. Temperature sensitivity of soil carbon decomposition and feedbacks to climate change. *Nature* 440: 165-173.

Denmead, O. T., and R. H. Shaw. 1962. Availability of soil water to plants as affected by soil moisture content and meteorological conditions. *Agronomy Journal* 54: 385-390.

Eastin, J. D., and C. Y. Sullivan. 1984. Environmental stress influences on plant persistence, physiology, and production. *In:* M. B. Tesar [ed.]. Physiological basis of crop growth and development. American Society of Agronomy and Crop Science Society of America, Madison, Wisconsin, p. 201-236.

Emmerich, W. E. 2003. Carbon dioxide fluxes in a semiarid environment with high carbonate

soils. *Agricultural and Forest Meeorology* 116: 91-102.

Falge, E., J. Tenhunen, D. Baldocchi, M. Aubinet, P. Bakwin, P. Berbigier, C. Bernhofer, J. M. Bonnefond, G. Burba, R. Clement, K. J. Davis, J. A. Elbers, M. Falk, A. H. Goldstein, A. Grelle, A. Granier, T. Grünwald, J. Gudmundsson, D. Hollinger, I. A. Janssens, P. Keronen, A. S. Kowalski, G. Katul, B. E. Law, Y. Malhi, T. Meyers, R. K. Monson, E. Moors, J. W. Munger, W. Oechel, K. T. P. U, K. Pilegaard, U. Rannik, C. Rebmann, A. Suyker, H. Thorgeirsson, G. Tirone, A. Turnipseed, K. Wilson, and S. Wofsy. 2002. Phase and amplitude of ecosystem carbon release and uptake potentials as derived from FLUXNET measurements. *Agricultural and Forest Meteorology* 113:75-95.

Farrell, A. E., M. O'Hare, D. M. Kammen, R. J. Plevin, B. T. Turner, and A. D. Jones. 2006. Ethanol can contribute to energy and environmental goals. *Science* 311:506-508.

Follett, R. F., J. M. Kimble, and R. Lal [eds.]. 2001. The potential of U.S. grazing lands to sequester carbon and mitigate the greenhouse effect. Lewis Publishers, Boca Raton, Florida.

Follett, R. F., and G. E. Schuman. 2005. Grazing land contributions to carbon sequestration. *In:* D. A. McGilloway [ed.]. Grassland: a global resource. Wageningen Academic Publishers, Wageningen, p. 265-277.

Funk, J. L., and M. T. Lerdau. 2004. Photosynthesis in forest canopies. *In:* M. D. Lowman and H. B. Rinker[eds.]. Forest canopies. Elsevier Academic Press, Amsterdam et al., p. 335-358.

Gilmanov, T. G., A. B. Frank, M. R. Haferkamp, T. P. Meyers, J. A. Morgan, L. L. Tieszen, B. K. Wylie, and L. B. Flanagan. 2005. Integration of CO_2 flux and remotely-sensed data for primary production and ecosystem respiration analyses in the Northern Great Plains:

Potential for quantitative spatial extrapolation. *Global Ecology and Biogeography* 14: 271-292.

Gilmanov, T. G., D. A. Johnson, and N. Z. Saliendra. 2003a. Growing season CO2 fluxes in a sagebrush-steppe ecosystem in Idaho: Bowen ratio/energy balance measurements and modeling. *Basic and Applied Ecology* 4: 167-183.

Gilmanov, T. G., D. A. Johnson, N. Z. Saliendra, K. Akshalov, and B. K. Wylie. 2004. Gross primary productivity of the true steppe in Central Asia in relation to NDVI: Scaling-up CO_2 fluxes. *Environmental Management* 39: S492-S508.

Gilmanov, T. G., J. F. Soussana, L. Aires, V. Allard, C. Ammann, M. Balzarolo, Z. Barcza, C. Bernhofer, C. L. Campbell, A. Cernusca, A. Cescatti, J. Clifton-Brown, B. O. M. Dirks, S. Dore, W. Eugster, J. Fuhrer, C. Gimeno, T. Gruenwald, L. Haszpra, A. Hensen, A. Ibrom, A. F. G. Jacobs, M. B. Jones, G. Lanigan, T. Laurila, A. Lohila, G.Manca, B. Marcolla, Z. Nagy, K. Pilegaard, K. Pinter, C. Pio, A. Raschi, N. Rogiers, M. J. Sanz, P. Stefani, M. Sutton, Z. Tuba, R. Valentini, M. L. Williams, and G. Wohlfahrt. 2007a. Partitioning European grassland net ecosystem CO2 exchange into gross primary productivity and ecosystem respiration using light response function analysis. *Agriculture, Ecosystems and Environment* 121: 93-120.

Gilmanov, T. G., T. J. Svejcar, D. A. Johnson, R. F. Angell, N. Z. Saliendra, and B. K. Wylie. 2006. Long-term dynamics of production, respiration, and net CO_2 exchange in two sagebrush-steppe ecosystems. *Rangeland Ecology and Management* 59: 585-599.

Gilmanov, T. G., S. B. Verma, P. L. Sims, T. P. Meyers, J. A. Bradford, G. G. Burba, and A. E. Suyker. 2003b. Gross primary production and light response parameters of four Southern Plains ecosystems estimated using long-term CO2-flux tower measurements - art. no.

1071. *Global Biogeochemical Cycles* 17: doi: 10.1029/2002GB002023, 2003.

Gilmanov, T. G., and WORLDGRASSAGRIFLUX Data Set Participants. 2007b. Productivity, respiration, CO2 sink potential, and light-response parameters of world grasslands derived from flux-tower data partitioning. *Eos Trans. AGU, 88(52), Fall Meet. Suppl., Abstract B32B-03.*

Good, N. E., and D. H. Bell. 1980. Photosynthesis, plant productivity and crop yield. *In:* P. S. Carlson, editor. The biology of crop productivity. Academic Press, New York, p. 3-51.

Goulden, M. L., J. W. Munger, S.-M. Fan, B. C. Daube, and S. C. Wofsy. 1996. Measurements of carbon sequestration by long-term eddy covariance: methods and critical evaluation of accuracy. *Global Change Biology* 2: 169-182.

Griffiths, H., and P. Jarvis [eds.]. 2005. The carbon balance of forest biomes. Taylor & Francis, New York et al.

Hollinger, S. E., C. J. Bernacchi, and T. P. Meyers. 2005. Carbon budget of mature no-till ecosystem in North Central Region of the United States. *Agricultural and Forest Meteorology* 130: 59-69.

Jarvis, P. G. 1994. Capture of carbon dioxide by a coniferous forest. *In:* J. L. Monteith, R. K. Scott, and M. H. Unsworth [eds.]. Resource capture by crops. Nottingham University Press, Loughborough, Leicestershire, p. 351-374.

King, A. W., L. Dilling, G. P. Zimmerman, D. M. Fairman, R. A. Houghton, G. Marland, A. Z. Rose, and T. J. Wilbanks, editors. 2007. The first state of the carbon cycle report (SOCCR): The North American carbon budget and implications for the global carbon cycle. A report by the U.S. Climate Change Science Program and the Subcommittee on Global Change Research. National Oceanic and Atmospheric Administration, National

Climatic Data Center, Asheville, NC, USA.

Körner, C. 2003. Slow in, rapid out – carbon flux studies and Kyoto target. *Science* 300:1242-1243.

Lal, R., J. M. Kimble, R. F. Follett, and C. V. Cole [eds]. 1998. The potential of U.S. cropland to sequester carbon and mitigate the greenhouse effect. Ann Arbor Press, Chelsea, MI.

Larcher, W. W. 1995. Physiological plant ecology: ecophysiology and stress physiology of functional groups. Springer-Verlag, Berlin ; New York.

Le Houèrou, H. N., and C. H. Hoste. 1977. Rangeland production and annual rainfall relations in the Mediterranean basin and in the African Sahelo-Sudanian Zone. *Journal of Range Management* 30: 181-189.

Lee, X., W. Massman, and B. Law [eds]. 2004. *Handbook of Micrometeorology: A Guide for Surface Flux Measurement and Analysis*. Kluwer Academic Publishers.

Lieth, H. 1975. Modeling the primary productivity of the world. *In*: H. Lieth, R. H. Whittaker [eds.]. Primary Productivity of the Biosphere. Springer-Verlag, New York, p. 237-263.

Loehle Enterprises. 2007. Global optimization 6.0. Global nonlinear optimization using Mathematica. Loehle Enterprises, Naperville, Illinois.

Long, S. P., M. B. Jones, and M. J. Roberts, eds. 1991. *Primary productivity of grass ecosystems of the tropics and sub-tropics*. Chapman & Hall, London; New York.

Mielnick, P. C., and W. A. Dugas. 2000. Soil CO_2 flux in a tallgrass prairie. *Soil Biology and Biochemistry* 32:221-228.

Mitscherlich, E. A. 1909. Das Gesetz des Minimums und das Gesetz des abnehmenden Bodenertrages. *Landwirtschaftliches Jahrbuch der Schweiz* 38: 537-552.

Moffat, A. M., D. Y. Hollinger, A. D. Richardson, A. G. Barr, C. Beckstein, B. H. Braswell, G.

Churkina, A. R. Desai, E. Falge, J. H. Gove, M. Heimann, D. Hui, A. J. Jarvis, J. Kattge, A. Noormets, V. J. Stauch, D. Papale, and M. Reichstein. 2007. Comprehensive comparison of gap-filling techniques for eddy covariance net carbon fluxes. *Agricultural and Forest Meteorology* 147: 209-232.

Monteith, J. L. 1972. Solar radiation and productivity in tropical ecosystems. *Journal of Applied Ecology* 9: 747-766.

Mordacq, L., J. Ghasghaie, and B. Saugier. 1991. A simple method for measuring the gas exchange of small trees. *Functional Ecology* 5:572-576.

Odum, E. P. 1959. Fundamentals of ecology. Philadelphia.

Odum, H. T. 1956. Primary production in flowing waters. *Limnology and Oceanography* 1:102-117.

Olson, J. S., J. A. Watts, and L. J. Allison. 1983. Carbon in live vegetation of major world ecosystems (Oak Ridge National Laboratory Technical Report ORNL-5862). Washington, D.C. U.S. Dept. of Energy, Springfield, Va.

Owen, K. E., E. Falge, R. Geyer, X. Xiao, P. Stoy, C. Ammann, A. Arain, M. Aubinet, M. Aurela, C. Bernhofer, B. H. Chojnicki, A. Granier, T. Gruenwald, J. Hadley, B. Heinesch, D. Hollinger, A. Knohl, W. Kutsch, A. Lohila, T. Meyers, E. Moors, C. Moureaux, K. Pilegaard, N. Saigusa, S. Verma, T. Vesala, C. Vogel, J. Tenhunen, M. Reichstein, and Q. Wang. 2007. Linking flux network measurements to continental scale simulations: Ecosystem carbon dioxide exchange capacity under non-water-stressed conditions. *Global Change Biology* 13:734-760.

Patzek, T. W., J. Lee, B. Li, J. Padnick, S. A. Yee, S. M. Anti, R. Campos, and K. W. Ha. 2005. Ethanol from corn: Clean renewable fuel for the future, or drain on our resources and

pockets? *Environment, Development and Sustainability* 7:319-336.

Powlson, D. S., A. B. Riche, and I. Shield. 2005. Biofuels and other approaches for decreasing fossil fuel emissions from agriculture. *Annals of Applied Biology* 146:193-201.

Rabinowich, E. I. 1951. Photosynthesis and related processes. Interscience Publishers, Inc, New York.

Reichstein, M., E. Falge, D. Baldocchi, D. Papale, R. Valentini, M. Aubinet, P. Berbigier, C. Bernhofer, N. Buchmann, M. Falk, T. Gilmanov, A. Granier, T. Grünwald, K. Havránková, D. Janous, A. Knohl, T. Laurela, A. Lohila, D. Loustau, G. Matteucci, T. Meyers, F. Miglietta, J.-M. Ourcival, D. Perrin, J. Pumpanen, S. Rambal, E. Rotenberg, M. Sanz, J. Tenhunen, G. Seufert, F. Vaccari, T. Vesala, and D. Yakir. 2005. On the separation of net ecosystem exchange into assimilation and ecosystem respiration: review and improved algorithm. *Global Change Bilology* 11: 1424-1439.

Reicosky, D. C. 1997. Tillage-induced CO_2 emission from soil. *Nutrient Cycling in Agroecosystems* 49:273-285.

Rodin, L. E., and N. I. Bazilevich. 1968. Production and mineral cycling in terrestrial vegetation. Oliver and Boyd, Edinburgh.

Rodin, L. E., N. I. Bazilevich, and N. N. Rozov. 1975. Productivity of the world's main ecosystems. *In*: D. E. Reichle, J. F. Franklin, and D. W. Goodall [eds.]. Productivity of the World Ecosystems. Proceedings, Symposium Fifth General Assembly of Special Committee of IBP. National Acad. of Sci., Washington, D.C., p. 13-26.

Rosenzweig, M. L. 1968. Net primary production of terrestrial communities: Prediction from climatological data. American Naturalist **102**:67-74.

Ruimy, A., P. G. Jarvis, and D. D. Baldocchi. 1995. CO_2 fluxes over plant canopies and solar

radiation: a review. *Anvances in Ecological Research* 26: 1-68.

Sala, O. E., W. J. Parton, L. A. Joyce, and W. K. Lauenroth. 1988. Primary production of the central grassland region of the United States. *Ecology* 69:40-45.

Singh, J. S., M. J. Trlica, P. G. Risser, R. E. Redmann, and J. K. Marshall. 1980. Autotrophic subsystem. Pages 59-200. In: A.I. Breymeyer and G. M. Van Dyne [eds.]. *Grasslands, systems analysis and man*. Cambridge University Press, Cambridge.

Slatyer, R. O. 1967. *Plant-water relationships*. Academic Press, London, New York.

Smith, P., and P. Falloon. 2005. Carbon sequestration in European croplands. Pages 47-55 *in* H. Griffiths and P. G. Jarvis, editors. The carbon balance of forest biomes. Taylor and Francis, New york.

Stoy, P. C., J. Y. Juang, K. A. Novick, J. M. Uebelherr, R. Oren, G. G. Katul, and M. B. S. Siqueira. 2006. An evaluation of models for partitioning eddy covariance-measured net ecosystem exchange into photosynthesis and respiration. *Agricultural and Forest Meteorology* 141: 2-18.

Tamiya, H. 1951. Some theoretical notes on the kinetics of algal growth. *Botanical Magazine* 6: 167-173.

Tarnocai, C., C.-L. Ping, and J. Kimble. 2007. Carbon cycle in the permafrost region of North America. Pages 127-138 in A. W. King, L. Dilling, G. P. Zimmerman, D. M. Fairman, H. R.A., G. Marland, R. A.Z., and T. J. Wilbanks, eds. *The First State of the Carbon Cycle Report (SOCCR): The North American Carbon Budget and Implications for the Global Carbon Cycle. A Report by the U.S. Climate Change Science Program and the Subcommittee on Global Change Research*. National Oceanic and Atmospheric Administration, National Climatic Data Center, Asheville, NC, USA.

Thornley, J. H. M., and I. R. Johnson. 2000. Plant and crop modelling. A mathematical approach to plant and crop physiology. The Blackburn Press, Caldwell, New Jersey.

Walter, H. 1939. Grassland, Savanne und Busch der ariden Teile Afrikas in ihrer ökologische Bedingtheit. *Jahrbuch fur wissenschaftliche Botanik* 87:850-860.

Weaver, J. E. 1924. Plant production as a measure of environments. *Journal of Ecology* 12: 205-237.

Whittaker, R. H., and G. E. Likens. 1973. Carbon in the biota. *In*: G. M. Woodwell and E. V. Pecan, eds. *Carbon and the biosphere*. National Technical Information Service, Springfield, Virginia, p. 281-302.

Wildung, R. E., T. R. Garland, and R. L. Buschbom. 1975. The interdependent effects of soil temperature and water content on soil respiration rate and plant root decomposition in arid grassland soils. *Soil Biology and Biochemistry* **7**:373-378.

Wolfram Research. 2009. www.wolfram.com.

Woodward, F. I., M. R. Lomas, and S. E. Lee. 2001. Predicting the future productivity and distribution of global terrestrial vegetation. *In:* J. Roy, B. Saugier, and H. A. Mooney [eds.]. Terrestrial global productivity. Academic Press, San Diego et al., p. 521-541.

Zhao, L., S. Gu, G. Yu, X. Zhao, Y. Li, S. Xu, and H. Zhou. 2006. Diurnal, seasonal and annual variation in net ecosystem CO2 exchange of an alpine shrubland on Qinghai-Tibetan plateau. *Global Change Biology* 12: 1940-1953.

Zhang, L.-M., Y. Gui-Rui, X.-M. Sun, X.-F. Wen, C.-Y. Ren, Y.-L. Fu, Q.-K. Li, Z.-Q. Li, Y.-F. Liu, D.-X. Guan, and J.-H. Yan. 2006. Seasonal variation of ecosystem apparent quantum yield (α) and maximum photosynthesis rate (Pmax) of different forest ecosystems in China. *Agricultural and Forest Meteorology* 137: 176-187.

FIGURES AND TABLES

Figure 1. Geographical distribution of the 118 nonforest flux tower sites considered in this study.

Figure 2. Major types of ecosystem light-response functions: A - linear, convexity $\theta = 1$ (corn crop, Bondville, IL, USA, 1999, day 188); B - nonrectangular hyperbolic, convexity $0 < \theta < 1$ (soybeans, Rosemount, MN, USA, 2004, day 207); C - rectangular hyperbolic, $\theta = 0$ (meadow bromegrass/alfalfa, Lacombe, Alberta, Canada, 2003, day 151); D - hysteresis (floodplain meadow, Cherskii, East Siberia, Russia, 2005, day 1900, $k_T = 0.056\ °C^{-1}$).

Figure 3. Light-temperature response surfaces fitted by modified nonrectangular equation [4] for representative days for: A - Doulun steppe, China, 2006, day 218; B – Brookings sown pasture, SD, USA, 2005, day 190; C – Howard wet-dry savanna, Australia, 2002, day 34; and D – Rondonia tropical grassland, Brazil, 1999, day 270.

Figure 4. Scatter diagrams of maximum weekly values of light-response (α, A_{max}, $P_{g,max}$, L_{max}), metabolic (r_d, $R_{e,max}$), and efficiency (ε, G_{max}) parameters for the pooled data set including grasslands (extensively and intensively managed), shrublands and savannas, wetlands, and croplands: A - α *vs* A_{max}; B – r_d *vs* A_{max}; C - ε *vs* A_{max}; D – A_{max} *vs* L_{max}; E – $P_{g,max}$ *vs* A_{max}; F – A_{max} *vs* G_{max}; G – $R_{e,max}$ *vs* $P_{g,max}$; and H - $P_{g,max}$ *vs* L_{max}. Dashed lines

describe linear or allometric equations characterizing patterns of co-variation between parameters.

Figure 5. Scatter diagrams of maximum weekly values of light-response *(α, A_{max}, $P_{g,max}$, L_{max})*, metabolic (r_d, $R_{e,max}$), and efficiency (ε, G_{max}) parameters for the extensively managed grasslands data subset: A - α *vs* A_{max}; B – r_d *vs* A_{max}; C - ε *vs* A_{max}; D – A_{max} *vs* L_{max}; E – $P_{g,max}$ *vs* A_{max}; F – A_{max} *vs* G_{max}; G – $R_{e,max}$ *vs* $P_{g,max}$; and H - $P_{g,max}$ *vs* L_{max}. Dashed lines describe linear or allometric equations characterizing patterns of co-variation between parameters.

Figure 6. Seasonal dynamics of light-response parameters: maximum photosynthesis, A_{max}, daytime ecosystem respiration, r_d, quantum yield, α, and gross ecological light-use efficiency, ε, in selected nonforest ecosystems: A – floodplain meadow, Cherskii, 2003; B – mixed prairie, Cottonwood, 2006; mixed prairie, Gudmundsen Ranch, 2006; D- tallgrass prairie, Fort Reno, 2005; E – wet-dry savanna, Howard, 2002; F – tropical grassland, Rondonia, 1999; G – sugar beet, Lonzee, 2004; H – corn crop, Bondville, 1999.

Figure 7. Seasonal dynamics and annual budgets of gross primary productivity, $P_g(t)$, total ecosystem respiration, $R_e(t)$, and cumulative net ecosystem CO2 exchange, *CumNEE(t)* for selected nonforest sites and years: A – floodplain meadow, Cherskii, 2003; B – sown northern temperate grassland, Jokioinen, 2001-2002; C – temperate grassland, Grillenburg, 2005; D – desert grassland, Audubon Ranch, 2004; E - dry

savanna, Skukuza, 2002; F – tropical grassland, Rondonia, 1999; G – corn crop, Bondville, 2003; H – soybean crop, Mead, 2002.

Figure 8. Frequency distributions of gross primary production (A), ecosystem respiration (B), and net ecosystem CO_2 exchange (C) estimates in the pooled set site-years from nonforest flux tower sites.

Figure 9. Scatter plot of *RE* versus *GPP* values for the pooled set of site-years from nonforest flux tower stations of the world. The 1:1 diagonal is shown as a dashed line.

Figure 10. Scatter plots of the *RE* versus *GPP* values for various types of nonforest ecosystems: A - extensively managed grasslands; B – intensively managed grasslands; C – shrublands and savanna; D – wetlands; E – croplands.

Figure 11. Histograms of statistical distributions of the annual net ecosystem CO_2 exchange values (*NEE*) in various types of nonforest ecosystems: A - extensively managed grasslands; B – intensively managed grasslands; C – shrublands and savanna; D – wetlands; E – croplands.

Figure 12. Response of gross primary production, *GPP*, (A, C) and ecosystem respiration, *RE*, (B, D) of extensively managed grasslands on the annual precipitation *PCPN* (A, B) and the dryness index $DI = R_{net}/(\lambda * PCPN)$. The dashed lines indicate nonlinear regressions describing predominant trends.

Figure 13. Response of gross primary production, *GPP*, (A, C) and ecosystem respiration, *RE*, (B, D) of intensively managed grasslands on the annual precipitation *PCPN* (A, B) and the dryness index $DI = R_{net}/(\lambda * PCPN)$. The dashed lines indicate nonlinear regressions describing predominant trends.

Figure 14. Response of gross primary production, *GPP*, (A, C) and ecosystem respiration, *RE*, (B, D) of shrublands and savanna on the annual precipitation *PCPN* (A, B) and the dryness index $DI = R_{net}/(\lambda * PCPN)$. The dashed lines indicate nonlinear regressions describing predominant trends.

Table 1. Nonforest flux tower sites analyzed in this study.

Site	Latitude	Longitude	Elevation	PCPN	Tyear	Years	Investigator(s)	Method*
				Croplands				
Ames, IA, USA, corn	41.720	-93.410	300	814	8.9	2003	J. Prueger	L
Auradé, France	43.549	1.108	243	690	13.3	2005	E. Ceschia, P. Beziat	T
Batavia-agro, IL, USA	41.859	-88.223	227	921	10.5	2005-2006	R. Matamala; D. Cook	T
Bondville, IL, USA, corn	40.006	-88.292	300	990	11.3	1997-2005	S. Hollinger; C. Bernacchi, T. Meyers	L
Bondville, IL, USA, soybeans	40.006	-88.292	300	990	11.3	1998-2006	S. Hollinger; C. Bernacchi, T. Meyers	L
Bondville-companion, IL, USA	40.006	-88.292	219	990	11.3	2005-2006	S. Hollinger; C. Bernacchi	T
Borgo Cioffi-crop, Italy	40.524	14.957	20	490	19.0	2004-2006	V. Magliulo	T
Carlow, Ireland	52.859	-6.918	59	824	9.4	2004-2006	M. Jones; G. Lanigan	L
Doulun, China	42.046	116.280	1350	399	3.3	2005-2006	Shiping Chen	L
Foulum-crop, Denmark	56.484	9.587	51	712	8.0	2005	J. Olesen; K. Schelde	T
Gebesee, Germany	51.100	10.914	162	492	9.6	2004-2006	C. Rebmann, W. Kutsch	T
Grignon, France	48.844	1.952	125	600	11.1	2005-2006	P. Cellier	T
Haller, PA, USA	48.860	-77.840	352	974	9.7	2003	R.H. Skinner	L

Klingenberg, Germany	50.893	13.222	480	850	7.0	2004-2006	C. Bernhofer; T. Gruenwald	T
Lamasquère, France, irrigated	43.493	1.237	180	690	13.3	2005	E. Ceschia	T
Langerak, France	52.004	4.806	-1	786	9.8	2005-2006	E. Moors, J. Elbers, W. Jans	T
Lonzee, Belgium	50.552	4.745	165	800	10.0	2004-2006	C. Moureaux, M. Aubinet	L
Mase, Japan, paddy field	36.054	140.027	13	1200	13.7	2002-2003	A. Miyata	T
Mead, NE, USA, corn rainfed	41.180	-96.440	363	887	9.7	2001-2003	S. Verma, A. Suyker	L
Meadm NE, USA, soybeans rainfed	41.180	-96.440	363	887	9.7	2002-2004	S. Verma, A. Suyker	L
Mead, maize rotation irrigated	41.165	-96.470	362	887	9.7	2001-2003	S. Verma, A. Suyker	T
Mead, NE, USA, corn irrigated	41.165	-96.477	361	728	10.1	2001-2004	S. Verma, A. Suyker	T
Mead, NE, USA, soybeans irrigated	41.165	-96.470	362	728	10.1	2002-2004	S. Verma, A. Suyker	T
Molenweg, Netherlands	51.650	4.639	1	800	9.8	2005	E. Moors, J. Elbers	T
Oensingen, Switzerland	47.286	7.734	452	1100	9.0	2005	N. Buchmann; W. Eugster	T
Ponca City, OK, USA, winter wheat	36.767	-97.133	310	866	14.8	1997	S. Verma	L
Risbyholm, Denmark	51.530	12.097	10	575	9.0	2004-2005	H. Soegaard	T
Rosemount, MN, USA	44.714	-93.090	260	799	6.8	2004-2005	T. Griffis, J. Baker	L
			Extensively managed grasslands					
Alinya, Spain	42.202	1.449	1770	669	13.0	2003-2005	M.J. Sanz	L
Amplero, Italy	41.867	13.633	884	1365	10.0	2003-2005	M. Balzarolo	L
Atquasuk, AK, USA	70.470	-157.409	N/A	127	NA?	1999-2006	W. Oechel	T
Audubon Ranch, AZ, USA	31.591	-110.510	985	382	16.0	2002-2006	T. Meyers	L
Barrow, AK, USA	71.323	-156.626	1	124	-12.5	1998-2002	W. Oechel	T
Batavia Prairie, IL, USA	41.841	-88.241	226	921	10.5	2005-2006	R. Matamala	L
Bily Kriz, Czech Republic	49.495	18.545	855	1200	5.5	2004-2006	M. Marek, R. Czerny	T
Brookings, SD, USA	44.311	-96.798	495	550	5.8	2004-2006	T. Meyers, T. Gilmanov, M. Heuer	L
Bugacpuszta, Hungary	46.800	18.900	100	500	10.8	2003-2006	Z. Tuba,	L
Canaan Valley, WV, USA	39.063	-79.421	988	900	8.2	2004	T. Meyers	L
Cheyenne, WY, USA	41.183	-104.900	1910	397	7.2	1997-1998	J. Morgan	L
Cottonwood, SD, USA	43.950	-101.847	735	447	7.7	2004-2006	T. Meyers, A. Detwyler, K. Brehe	L
CPER, CO, USA	40.683	-104.750	1660	332	9.2	2001-2004	J. Morgan	L
Doulun, China	42.047	116.284	1350	399	3.3	2006	Shiping Chen	L
Duke grassland, NC, USA	35.971	-79.090	163	1145	15.5	2001-2005	G. Katul	L
Fort Peck, MT, USA	48.308	-105.101	634	310	7.7	2000-2006	T. Meyers	L
Fort Reno, OK, USA	35.557	-98.017	421	870	14.9	2005	M. Torn, D. Billesbach	L
Freeman Ranch, TX, USA	29.930	-98.010	244	959	19.4	2004	J. Heilman	L

Goodwin Creek, MS, USA	34.250	-89.970	70	1455	15.7	2002-2006	T. Meyers	L
Grillenburg, Germany	50.951	13.514	400	853	7.2	2004-2006	C. Bernhofer, T. Gruenwald	L
Gudmundsen Ranch, NE, USA	42.069	-101.407	1081	560	7.9	2006	D. Billesbach	L
Haibei, China	37.617	101.317	3250	561	-1.7	2002-2003	T. Kato	T
Ivotuk, Alaska	68.486	-155.750	550	250	-9.0	2004-2006	W. Oechel	T
Jornada, NM, USA	32.600	-106.750	1320	272	N/A	2000-2001	W. Dugas, P. Mielnick	L
Karnap, Uzbekistan	40.000	65.500	310	237	14.6	2001	M. Nasyrov, N. Saliendra	L
Kendall, AZ, USA	31.737	-109.942	1531	356	17.0	1999-2006	W. Emmerich	L
Khakasia, Russia	54.773	90.002	430	304	0.5	2002-2004	L. Belelli	L
Khakasia-3, Russia	54.705	89.078	N/A	N/A	N/A	2004	L. Belelli	T
Kherlenbayan, Mongolia	47.214	108.737	1235	196	1.2	2003	S. Li	L
Laqueuille, France	45.643	2.736	1040	1013	8.6	2002-2006	J.-F. Soussana, V. Allard	L
Lethbridge, Canada	49.709	-112.940	960	378	6.4	1998-2002	L. Flanagan	L
Little Washita, OK, USA	34.967	-97.983	335	750	16.3	1997-1998	T. Meyers	L
Malga Arpaco, Italy	46.117	11.703	1699	1200	6.3	2003-2004	A. Raschi	L
Mandan, ND, USA	46.767	-100.917	518	404	5.0	1999-2001	A. Frank	L
Matra, Hungary	47.842	19.726	350	605	10.6	2004-2005	J. Balogh	T
Miles City, MT, USA	46.300	-105.967	719	343	7.9	2000-2001	M. Haferkamp	L
Monte Bondone, Italy	46.016	11.047	1550	1189	5.5	2003-2006	D. Gianelle	T
Neal Smith, IA, USA	41.558	-93.296	280	826	9.1	2005	J. Prueger	L
Neustift, Austria	47.117	11.317	970	850	6.3	2001-2006	G. Wohlfahrt	L
Oensingen, Switzerland	47.283	7.733	450	1100	9.0	2002-2003	C. Ammann, J. Fuhrer	L
Rannels Ranch, KS, USA	39.139	-96.523	324	840	12.9	1998-1999	C. Owensby	L
Rigi-Seebodenalp, Switzerland	47.058	8.457	1025	1327	7.3	2003	W. Eugster, N. Rogiers	L
Rondonia, Brazil	-10.762	-62.357	306	1664	23.9	1999	M. Waterloo, A. Manzi	L
Santarem, Brazil	-3.012	-54.537	N/A	N/A	N/A	2001-2002	D. Fitzjarrald	L
Shidler, OK, USA	36.933	-96.683	356	942	14.8	1997-1999	S. Verma, A. Suyker	L
Shortandy, Kazakhstan	51.667	71.000	367	323	1.6	1998-2001	K. Akshalov, N. Saliendra, D. A. Johnson	L
Temple, TX, USA	31.100	-97.333	219	878	19.6	1998-1999	W. Dugas, P. Mielnick	L
Tojal, Portugal	38.477	-8.025	190	750	15.5	2004-2006	C. Pio, L. Aires	L
Viara Ranch, CA, USA	38.407	-120.951	129	500	15.9	2001-2006	D. Baldocchi	L
Walnut River, KS, USA	37.521	-96.855	408	1030	13.1	2002-2004	R. Coulter, D. Cook	L
Woodward, OK, USA	36.600	-99.583	630	586	14.3	1997-2002	P. Sims, J. Bradford	L
Xilinhot grazed, China	43.554	116.671	1250	360	2.0	2006	Shiping Chen	L
Xilinhot-fenced, China	43.546	116.678	1250	360	2.0	2006	Shiping Chen	T
Xilinhot-typical fenced, China	44.134	116.329	1030	290	2.0	2004-2006	Guangsheng Zhou	T

Intensively managed grasslands								
Cabauw- extension. The Netherlands	51.954	4.903	-1	786	9.8	2005	E. Moors, J. Elbers	T
Cabauw, The Netherlands	51.967	4.917	-1	800	10.0	2003	A. Hensen	T
Cabauw, The Netherlands	51.971	4.927	-1	786	9.8	2004-2006	E. Moors, J. Elbers	T
Carlow-grassland, Ireland	52.850	-6.900	50	804	10.1	2003	M. Jones, G. Lanigan	L
Dripsey-grass, Ireland	51.919	-8.751	187	1450	9.5	2002-2005	G. Kiely, P. Leahy	T
Easter Bush, UK	55.867	-3.200	190	890	8.0	2003-2004	M. Sutton	L
Haarweg, The Netherlands	51.970	5.630	7	760	9.5	2002	A. Jacobs	T
Haastrect, Netherlands	52.004	4.806	-2	786	9.8	2003	E. Moors	T
Haller, PA, USA	40.862	-77.840	352	974	9.7	2003-2005	R.H. Skinner	L
Hegihátsál, Hungary	46.950	16.650	248	759	8.9	1999	Z. Barcza, L. Haszpra	T
Horstermeer, Netherlands	52.029	5.068	-2	797	9.8	2004-2006	H. Dolman	T
Jokioinen, Finland	60.899	23.514	104	581	3.9	2002	A. Lohila, T. Laurila	L
Lacombe, Canada	52.436	-113.808	871	446	2.1	2003	V.S. Baron	L
Laqueuille, France	45.643	2.736	1040	1013	8.6	2002-2006	J.-F. Soussana, V. Allard	L
Lelystad, The Netherlands	52.500	5.500	0	780	10.0	2004	A. Hensen	L
Lille Valby, Denmark	55.700	12.117	15	1119	8.5	2004-2006	E. Dellwik	L
Oensingen, Switzerland	47.283	7.733	450	1100	9.0	2002-2006	C. Ammann; J. Fuhrer	L
Shrublands and savanna								
Burns, OR, USA	43.483	-119.717	1380	283	7.6	1995-2001	T. Svejcar	L
Dubois, ID, USA	44.267	-112.133	1700	302	6.2	1996-2001	N. Saliendra, D.A. Johnson	L
Howard Springs, Australia	-12.329	131.000	38	1824	25.9	2002-2005	J. Berringer	L
Karrykul, Turkmenistan	38.600	58.400	90	148	15.6	1998-2000	M. Dourikov, N. Saliendra, D.A. Johnson	L
Kubuqi, China	40.381	108.549	1160	180	7.5	2006	Shiping Chen	L
Santa Rita, AZ, USA	31.821	-110.866	1120	330	17.6	2004-2006	R. Scott	T
Sao Paulo, Brazil	-21.619	-47.650	N/A	953	N/A	2001-2002	H. da Rocha	T
Skukuza, South Africa	-24.983	31.600	263	561	21.6	2001-2003	N. Hanan	L
Sky Oaks, CA, USA, old stand	33.374	-116.623	1394	491	12.2	1997-2006	W. Oechel	L
Sky Oaks, CA, USA, young stand	33.377	-116.623	1429	491	12.2	1997-2001	W. Oechel	T
Tonzi Ranch, CA, USA	38.432	-120.966	177	559	15.4	2002-2006	D. Baldocchi	T
Wetlands								
Cherskii, Russia	68.615	161.339	4	200	-12.5	2003-2004	C. Corradi	T
CzechWet, Czech Republic	49.025	14.772	420	740	7.2	2006	M. Marek; D. Janous	T
Dongtan marsh-1, China	31.517	121.961	31	2192	15.7	2005	Bin Zhao; Guo Haiquang	T
Dongtan marsh-2,	31.585	121.903	31	2074	15.7	2005	Bin Zhao; Guo	T

China							Haiquang	
Dongtan marsh-3, China	31.517	121.972	31	1957	15.5	2005	Bin Zhao; Guo Haiquang	T
Kaamanen wetland, Finland	69.141	27.295	155	395	-1.3	2000-2006	T. Laurila; M. Aurela	T
PolWet, Poland	52.762	16.309	54	550	8.1	2004	J. Olejnik	T
Siikaneva, Finland	61.833	24.193	N/A	713	3.0	2004-2006	M. Aurela	T
Tadham Moore, UK	51.207	-2.829	3	750	11.1	2001	R. Harding	T

* Method on net flux partitioning into photosynthesis and respiration: L – light-response function analysis; T – nighttime temperature dependence.

Table 2. Parameters α, A_{max}, r_d, and θ from the nonrectangular hyperbolic light-response function $F_c(Q) = \frac{1}{2\theta}\left(\alpha Q + A_{max} - \sqrt{(\alpha Q + A_{max})^2 - 4\alpha A_{max}\theta Q}\right) - r_d$, for representative days at the Bondville, Rosemount, Lacombe, and Brookings flux tower stations.

Statistical characteristics	Parameters			
	Slope, α mg CO_2 μmol^{-1}	Plateau, A_{max} mg CO_2 m^{-2} s^{-1}	Respiration, r_d mg CO_2 m^{-2} s^{-1}	Convexity, θ dimensionless
A. Corn crop, Bondville, IL, USA, 1999, day 188 R^2 = 0.98; SE = 0.158 mg CO_2 m^{-2} s^{-1}				
Estimate	0.0014	3.2	0.1936	1.0
Standard Error	0.0001	-	0.0423	0.0012
Student's *t*	19.92	-	4.58	84.20
p-level	0.0000	-	0.0000	0.0000
Soybeans, Rosemount, MN, USA, 2004, day 207 R^2 = 0.98; SE = 0.045 mg CO_2 m^{-2} s^{-1}				
Estimate	0.0009	0.9930	0.2002	0.6947
Standard Error	0.0002	0.1899	0.0221	0.3329
Student's *t*	4.77	5.23	9.07	2.09
p-level	0.0000	0.0000	0.0000	0.0243
Sown pasture, Lacombe, Alberta, Canada, 2003, day 151 R^2 = 0.94; SE = 0.061 mg CO_2 m^{-2} s^{-1}				

Estimate	0.0026	0.8321	0.3413	0.0
Standard Error	0.0009	0.0969	0.0273	-
Student's *t*	2.98	8.58	12.50	-
p-level	0.0023	0.0000	0.0000	-
Floodplain meadow, Cherskii, East Siberia, Russia, 2003, day 214 $R^2 = 0.93$; SE = 0.033 mg CO_2 m^{-2} s^{-1}				
Estimate	0.0006	0.2987	0.1038	0.9333
Standard Error	0.0001	0.0252	0.090	0.090
Student's *t*	5.31	11.85	11.58	10.38
p-level	0.0000	0.0000	0.0000	0.0000

1

2

3 Table 3. Parameters α, A_{max}, r_0, k_T and θ from the modified nonrectangular hyperbolic

4 light-temperature response function

5 $F_C(Q, T_s) = \frac{1}{2\theta}\left(\alpha Q + A_{\max} - \sqrt{(\alpha Q + A_{\max})^2 - 4\alpha A_{\max}\theta Q}\right) - r_0 e^{k_T T_s}$, for

6 representative days at Doulun, Brookings, Howard, and Rondonia sites.

7

Statistical characteristics	Parameters				
	Slope, α mg CO_2 µmol^{-1}	Plateau, A_{max} mg CO_2 m^{-2} s^{-1}	Respiration, r_0 mg CO_2 m^{-2} s^{-1}	Temperature coefficient, k_T, $(°C)^{-1}$	Convexity, θ dimensionless
A. Steppe, Doulun, China, 2006, day 218 $R^2 = 0.98$; SE = 0.037 mg CO_2 m^{-2} s^{-1}					
Estimate	0.0009	0.5542	0.0377	0.0671	0.9644
Standard Error	0.00001	0.0241	0.0102	0.0116	0.0408
Student's *t*	9.08	22.98	3.68	5.78	23.64
p-level	0.0000	0.0000	0.0003	0.0000	0.0000
B. Sown pasture, Brookings, SD, USA, 2005, day 190 $R^2 = 0.99$; SE = 0.032 mg CO_2 m^{-2} s^{-1}					
Estimate	0.0014	1.0867	0.0631	0.0614	0.0000
Standard Error	0.0001	0.0498	0.0141	0.0094	0.0000
Student's *t*	13.87	21.81	4.48	6.53	-
p-level	0.0000	0.0000	0.0000	0.0000	-
C. Wet-dry savanna, Howard, Australia, 2002, day 34 $R^2 = 0.97$; SE = 0.074 mg CO_2 m^{-2} s^{-1}					
Estimate	0.0017	1.147	0.0278	0.0690	0.8376
Standard Error	0.0003	0.1019	0.0167	0.0186	0.1529
Student's *t*	5.83	11.25	1.67	3.71	5.48

p-level	0.0000	0.0000	0.0522	0.0004	0.0000
D. Tropical grassland, Rondonia, Brazil, 1999, day 270 $R^2 = 0.97$; SE = 0.052 mg CO_2 m^{-2} s^{-1}					
Estimate	0.0008	0.8048	0.0339	0.0760	0.9902
Standard Error	0.0001	0.0721	0.0183	0.0217	0.0230
Student's *t*	9.38	11.16	1.85	3.50	43.04
p-level	0.0000	0.0000	0.0408	0.0014	0.0000

* Not significantly different from zero

Table 4. Statistical characteristics of annual gross primary production (*GPP*), total ecosystem respiration (*RE*), and net ecosystem exchange (*NEE*) for major groups within nonforest terrestrial ecosystems.

	Ecosystem group				
Statistical characteristics	Grasslands extensively managed	Grasslands intensively managed	Shrublands and savanna	Wetlands	Croplands
Gross primary production, GPP (g CO_2 m^{-2} yr^{-1})					
Number of site-years	179	34	28	48	66
Mean	2708	5767	2949	2328	4521
Standard deviation	1842	1144	1950	1836	1365
Minimum	95	3141	645	749	1376
Maximum	8600	7720	6836	5643	6774
Total ecosystem respiration, RE (g CO_2 m^{-2} yr^{-1})					
Number of site-years	169	34	27	18	66
Mean	2535	4990	2537	1824	3588
Standard deviation	1689	1024	1396	1373	909
Minimum	112	3186	756	665	1052
Maximum	7880	7003	5094	4751	5905
Net Ecosystem Exchange, NEE (g CO_2 m^{-2} yr^{-1})					
Number of site-years	169	36	27	18	66
Mean	239	848	493	504	933
Standard deviation	521	658	740	719	814
Minimum	-1342	-961	-585	-40	-770
Maximum	1762	2934	2254	2226	2382

Table 5. Maximum values of daytime gross primary productivity, $P_{g,max}$, and annual net primary production, *GPP*, estimated for nonforest and forest flux-tower sites

Site	Year	$P_{g,max}$	Site	Year	*GPP*

		g CO_2 m^{-2} d^{-1}			g CO_2 m^{-2} yr^{-1}
A. Grasslands extensively managed					
Neustift, Austria	2004	76.2	Rondonia, Brazil	1999	**8600**
Jornada, NM, USA	2000	63.1	Neustift, Austria	2006	7415
Rannels Ranch, KS, USA	1998	60.8	Goodwin Creek, MS, USA	2004	6391
Batavia Prairie Site, IL, USA	2006	59.9	Grillenburg, Germany	2005	6299
Grillenburg, Germany	2005	57.34	Duke grassland, NC, USA	2003	6039
Monte Bondone, Italy	2006	56.9	Laqueuille, France, extensive	2006	5943
Shidler, OK, USA	1999	56.9	Neal Smith, IA, USA	2005	5756
Temple, TX, USA	1999	56.2	Batavia Prairie Site, IL, USA	2006	5435
Oensingen, Switzerland	2003	53.6	Oensingen, Switzerland	2003	5326
Neal Smith, IA, USA	2005	52.7	Laqueuille, France, extensive	2004	5322
Laqueuille, France, extensive	2004	51.7	Rigi-Seebodenalp, Switzerland	2003	5320
Goodwin Creek, MS, USA	2003	51.4	Shidler, OK, USA	1997	5208
B. Grasslands intensively managed					
Cabauw- extension. The Netherlands	2005	76.3	Oensingen, Switzerland	2004	7720
Easter Bush, UK	2003	63.6	Dripsey-grass, Ireland	2004	7388
Oensingen, Switzerland	2004	63.5	Haastrect, Netherlands	2003	7267
Lille Valby, Denmark	2006	63.4	Lille Valby, Denmark	2004	6873
Haastrect, Netherlands	2003	63.1	Laqueuille, France, intensive	2004	6838
Laqueuille, France, intensive	2006	59.0	Carlow-grassland, Ireland	2003	6807
Carlow-grassland, Ireland	2003	57.9	Easter Bush, UK	2003	6793
Haarweg, The Netherlands	2002	57.5	Cabauw- extension. The Netherlands	2005	6785
Dripsey-grass, Ireland	2003	54.7	Haarweg, The Netherlands	2002	5915
Lacombe, Alberta, Canada	2003	53	Hegihátsál, Hungary	1999	5867
Haller, State College, PA, USA	2004	52.2	Cabauw, The Netherlands	2004	5837
Cabauw, The Netherlands	2004	47.9	Horstermeer, Netherlands	2006	5337
C. Shrubs and savannas					
Howard Springs, Australia	2005	54.2	Sao Paulo cerrado, Brazil	2002	6836
Sao Paulo cerrado, Brazil	2002	42.7	Howard Springs, Australia	2002	5874
Tonzi Ranch, California	2005	38.6	Skukuza, South Africa	2001	3947
Skukuza, South Africa	2001	34.6	Tonzi Ranch, CA, USA	2005	3837

Tonzi Ranch, California	2003	34.1	Sky Oaks Old stand, CA, USA	1997	2682
Sky Oaks Young stand, CA, USA	1998	22.7	Sky Oaks Young stand, CA, USA	1998	2021
Sky Oaks Old stand, CA, USA	1997	21.0	Skukuza, South Africa	2003	1873
Santa Rita mesquite, AZ, USA	2005	19.8	Santa Rita mesquite, AZ, USA	2005	1125
Kubuqi, shrubland, China	2006	12.8	Kubuqi, shrubland, China	2006	1021
Karrykul, Turkmenistan	2000	7.79	Karrykul, Turkmenistan	2000	769
D. Wetlands					
Dongtan marsh-2, China	2005	70.1	Dongtan marsh-2, China	2005	5643
CzechWet, Czech Republic	2006	56.9	CzechWet, Czech Republic	2006	5368
Dongtan marsh-1, China	2005	51.9	Dongtan marsh-1, China	2005	5150
Dongtan marsh-3, China	2005	43.3	Tadham Moore, UK	2001	4767
Tadham Moore, UK	2001	41.1	Dongtan marsh-3, China	2005	3662
PolWet, Poland	2005	41.1	PolWet, Poland	2005	3393
Cherskii, Russia	2003	20.1	Siikaneva, Finland	2005	1359
Kaamanen wetland, Finland	2005	19.8	Kaamanen wetland, Finland	2005	1210
Siikaneva, Finland	2004	19.8	Cherskii, Russia	2003	834
E. Croplands					
Mead, corn rot. irrigated, NE, USA	2001	**116.1**	Langerak-crop, France	2005	6774
Mead, maize cont. irrigated, NE, USA	2001	**107.8**	Mead, rot. corn irrigated, NE, USA	2003	6720
Bondville, corn, IL, USA	1999	**99.9**	Borgo Cioffi-crop, Italy	2005	6513
Batavia-agro, IL, USA	2006	**99.0**	Mead, cont. corn irrigated, NE, USA	2001	6437
Bondville, corn, IL, USA	1999	94.1	Borgo Cioffi-crop, Italy	2006	6393
Borgo Cioffi-crop, Italy	2006	93.1	Mead, maize rotation irrigated	2001	6316
Mead, corn rainfed, NE, USA	2003	87.6	Lonzee, Belgium, sugar beet	2005	6313
Langerak-crop, France	2006	87.5	Oensingen-crop, Switzerland	2005	6295
Bondville-companion, IL, USA	2006	83.03	Mead corn rainfed, NE, USA	2001	5834
Grignon-crop, France	2005	81.3	Bondville, corn, IL, USA	1999	5602
Lonzee, winter wheat, Belgium	2005	80.5	Bondville, soybeans, IL, USA	2005	5582
Bondville, soybeans, IL, USA	2005	80.1	Risbyholm, Denmark, crop	2004	5525
F. Forests and plantations					
Duke Forest Loblolly Pine, NC, USA	2001	**99.0**	French Guyana	2004	**14339**
Campbell River, British Columbia, Canada	1998	86.6	Vanuatu - CocoFlux	2002	13057
Hampshire Forest, UK	2004	73.9	Rondonia forest, Brazil	2002	12727
Duke Forest Loblolly Pine	2005	69.0	Palangkaraya, Indonesia	2003	12236

Vanuatu - CocoFlux	2003	68.2	Santarem km67 primary forest, Brazil	2003	11703
Duke Forest Hardwood, NC, USA	2003	67.6	Caxiuana Forest-Almeirim, Brasil	2002	11436
French Guyana	2005	64.21	Santarem km67 primary forest, Brazil	2002	11271
Rondonia forest, Brazil	2002	60.8	Loblolly Pine plantation, NC, USA	2006	10173
Campbell River, British Columbia, Canada	2000	60.1	Donaldson Slash Pine Plantation, FL, USA	1999	9249
Loblolly Pine plantation, NC, USA	2006	59.7	Campbell River, British Columbia, Canada	2005	9162
Duke Forest Hardwood, NC, USA	2004	57.5	Duke Forest Loblolly Pine, NC, USA	2002	9067
Donaldson Slash Pine Plantation, FL, USA	1999	54.6	Duke Forest Hardwood, NC, USA	2003	8892

1

2

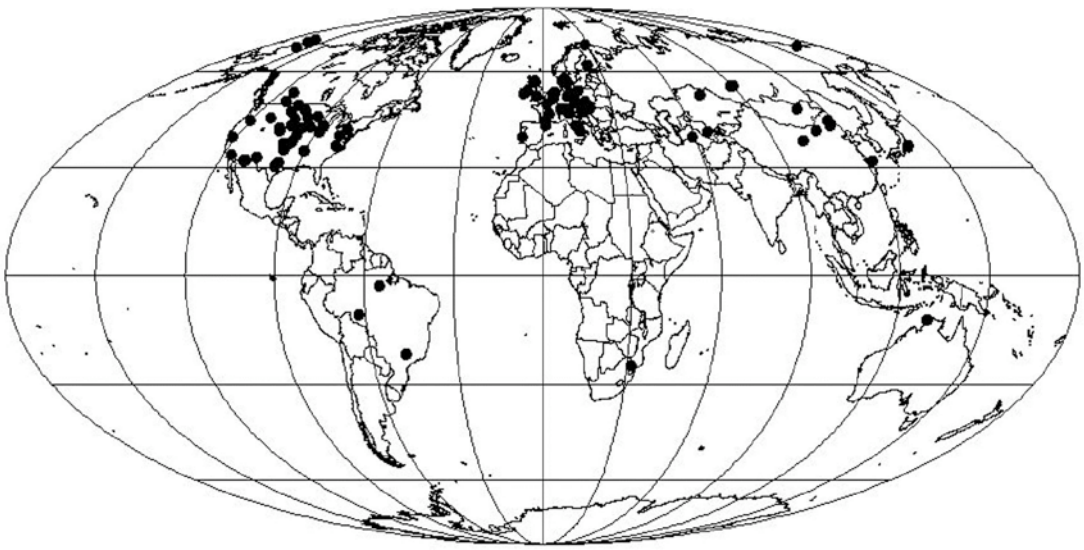

1

2 **Figure 1.**

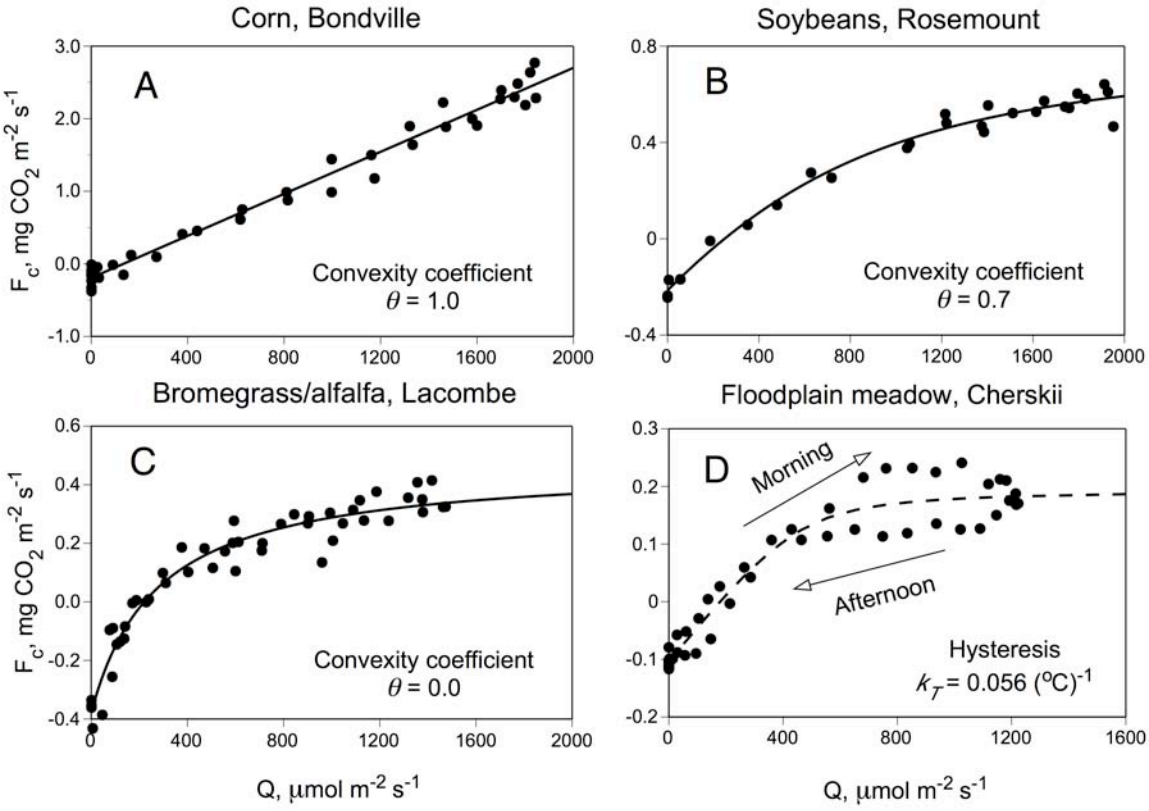

3

4 **Figure 2.**

5

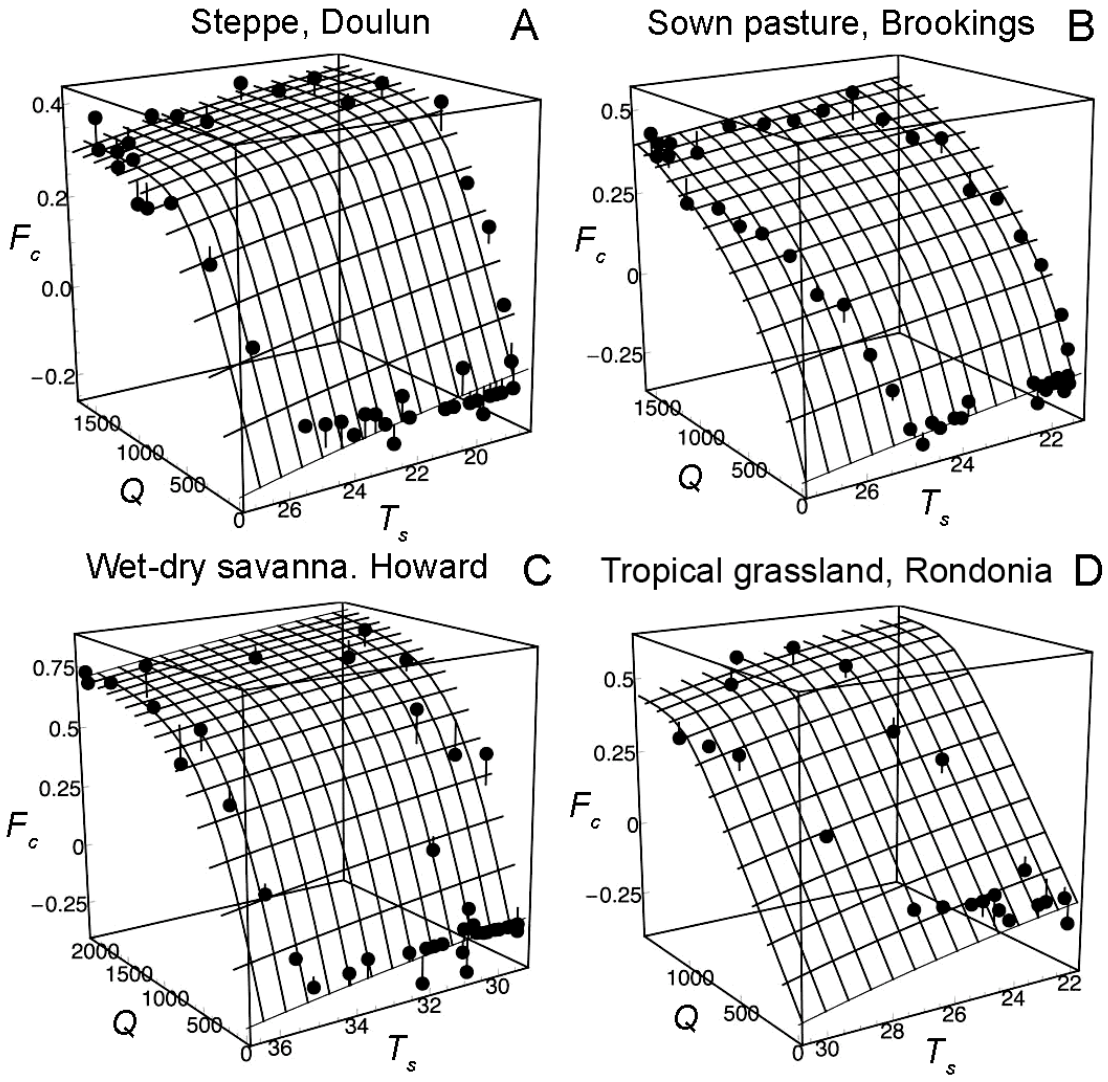
Steppe, Doulun
A
Sown pasture, Brookings
B
Wet-dry savanna. Howard
C
Tropical grassland, Rondonia
D
F_c
Q
T_s

1

2 **Figure 3.**

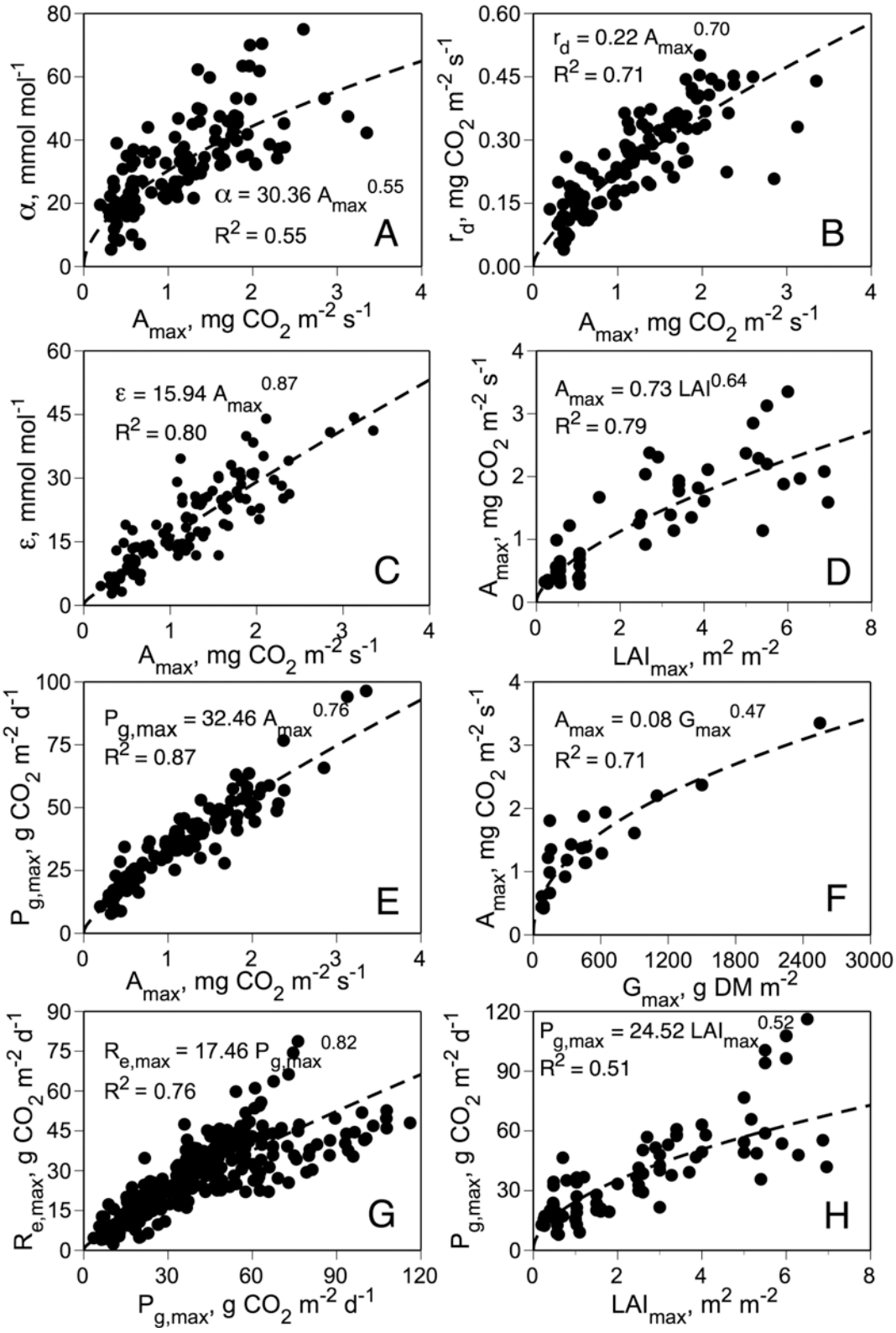
α, mmol mol-1
α = 30.36 Amax 0.55
R2 = 0.55
A
Amax, mg CO2 m-2 s-1
rd, mg CO2 m-2 s-1
rd = 0.22 Amax 0.70
R2 = 0.71
B
ε, mmol mol-1
ε = 15.94 Amax 0.87
R2 = 0.80
C
Amax = 0.73 LAI0.64
R2 = 0.79
D
LAImax, m2 m-2
Pg,max, g CO2 m-2 d-1
Pg,max = 32.46 Amax 0.76
R2 = 0.87
E
Amax = 0.08 Gmax 0.47
R2 = 0.71
F
Gmax, g DM m-2
Re,max, g CO2 m-2 d-1
Re,max = 17.46 Pg,max 0.82
R2 = 0.76
G
Pg,max, g CO2 m-2 d-1
Pg,max = 24.52 LAImax 0.52
R2 = 0.51
H

Figure 4.

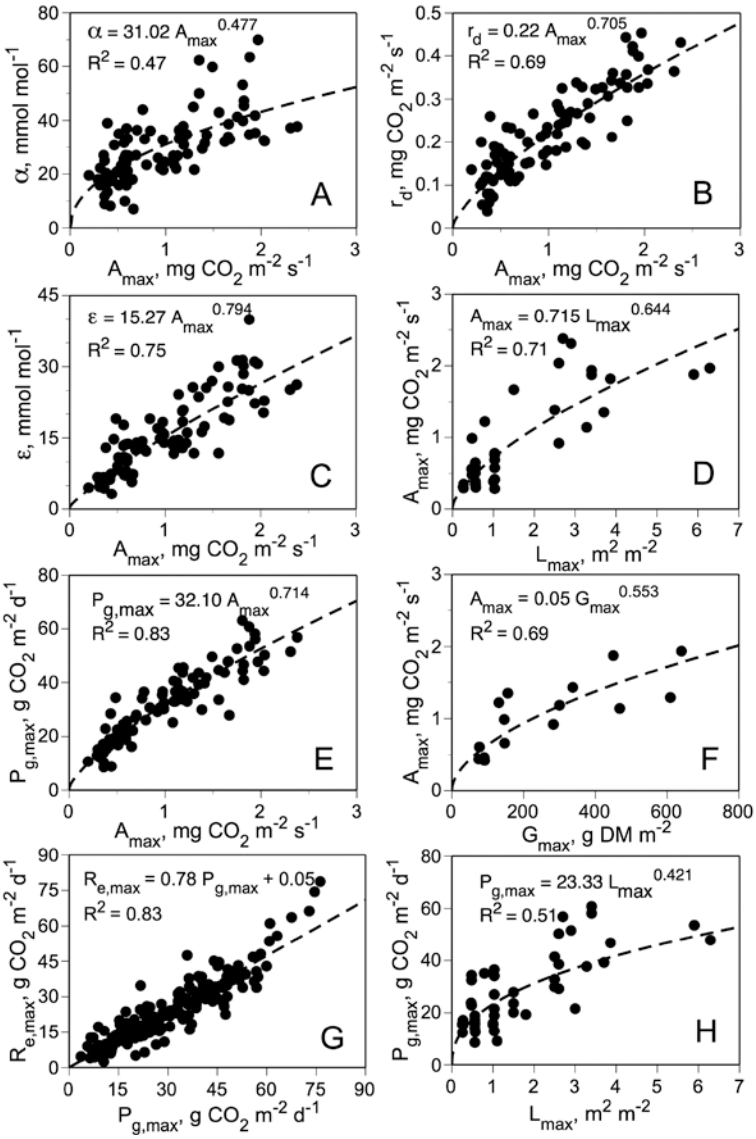
α = 31.02 A_max^0.477
R² = 0.47
α, mmol mol⁻¹
A_max, mg CO2 m⁻² s⁻¹
A
r_d = 0.22 A_max^0.705
R² = 0.69
r_d, mg CO2 m⁻² s⁻¹
A_max, mg CO2 m⁻² s⁻¹
B
ε = 15.27 A_max^0.794
R² = 0.75
ε, mmol mol⁻¹
A_max, mg CO2 m⁻² s⁻¹
C
A_max = 0.715 L_max^0.644
R² = 0.71
A_max, mg CO2 m⁻² s⁻¹
L_max, m² m⁻²
D
P_g,max = 32.10 A_max^0.714
R² = 0.83
P_g,max, g CO2 m⁻² d⁻¹
A_max, mg CO2 m⁻² s⁻¹
E
A_max = 0.05 G_max^0.553
R² = 0.69
A_max, mg CO2 m⁻² s⁻¹
G_max, g DM m⁻²
F
R_e,max = 0.78 P_g,max + 0.05
R² = 0.83
R_e,max, g CO2 m⁻² d⁻¹
P_g,max, g CO2 m⁻² d⁻¹
G
P_g,max = 23.33 L_max^0.421
R² = 0.51
P_g,max, g CO2 m⁻² d⁻¹
L_max, m² m⁻²
H

Figure 5.

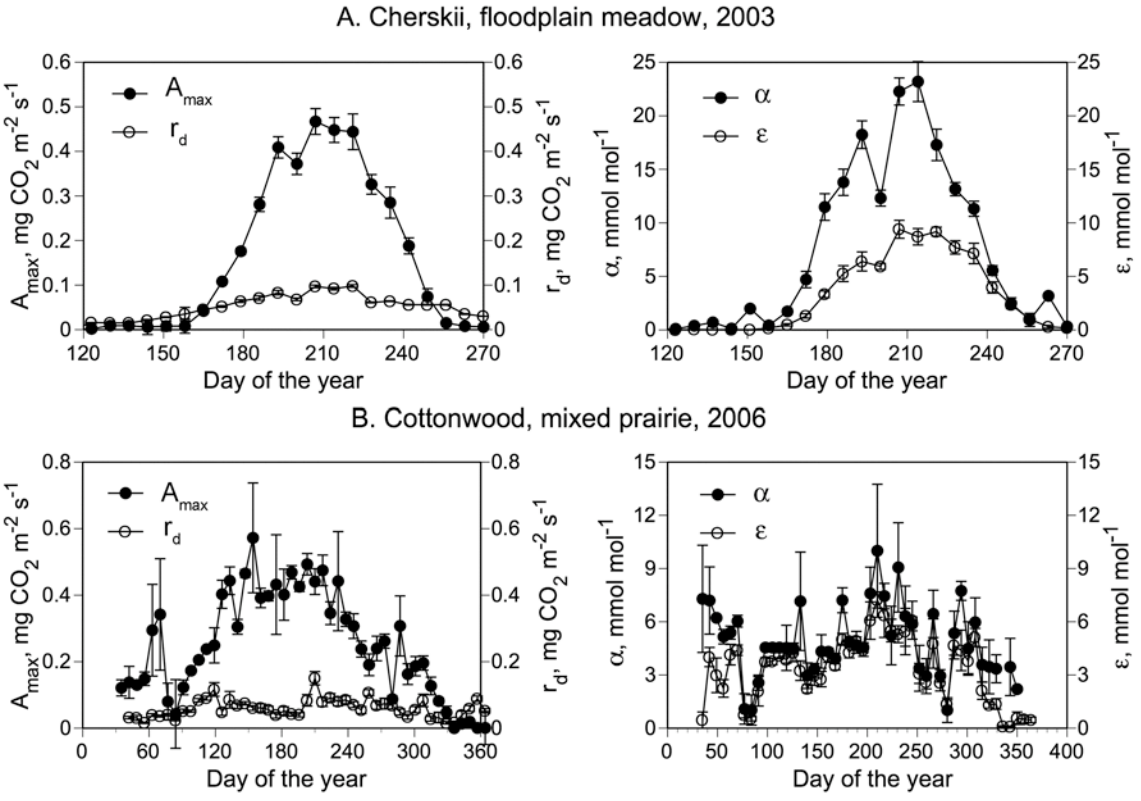
A. Cherskii, floodplain meadow, 2003
B. Cottonwood, mixed prairie, 2006
C. Gudmundsen, mixed prairie, 2006
D. Fort Reno, tallgrass prairie, 2005
A_max
r_d
α
ε
A_max, mg CO2 m-2 s-1
r_d, mg CO2 m-2 s-1
α, mmol mol-1
ε, mmol mol-1
Day of the year

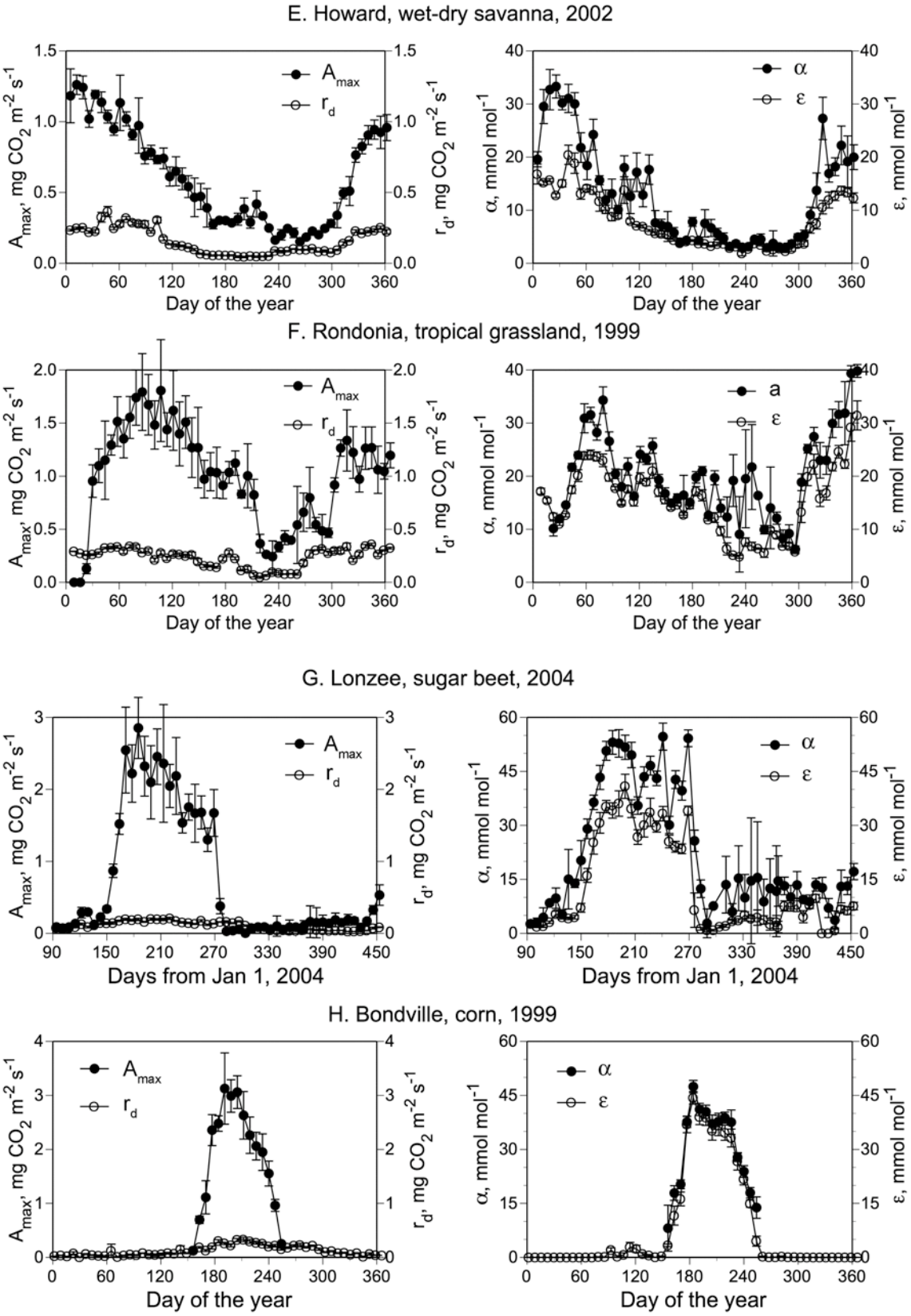
E. Howard, wet-dry savanna, 2002
F. Rondonia, tropical grassland, 1999
G. Lonzee, sugar beet, 2004
H. Bondville, corn, 1999
A_max
r_d
α
ε
a
A_max, mg CO2 m-2 s-1
r_d, mg CO2 m-2 s-1
α, mmol mol-1
ε, mmol mol-1
Day of the year
Days from Jan 1, 2004

Figure 6.

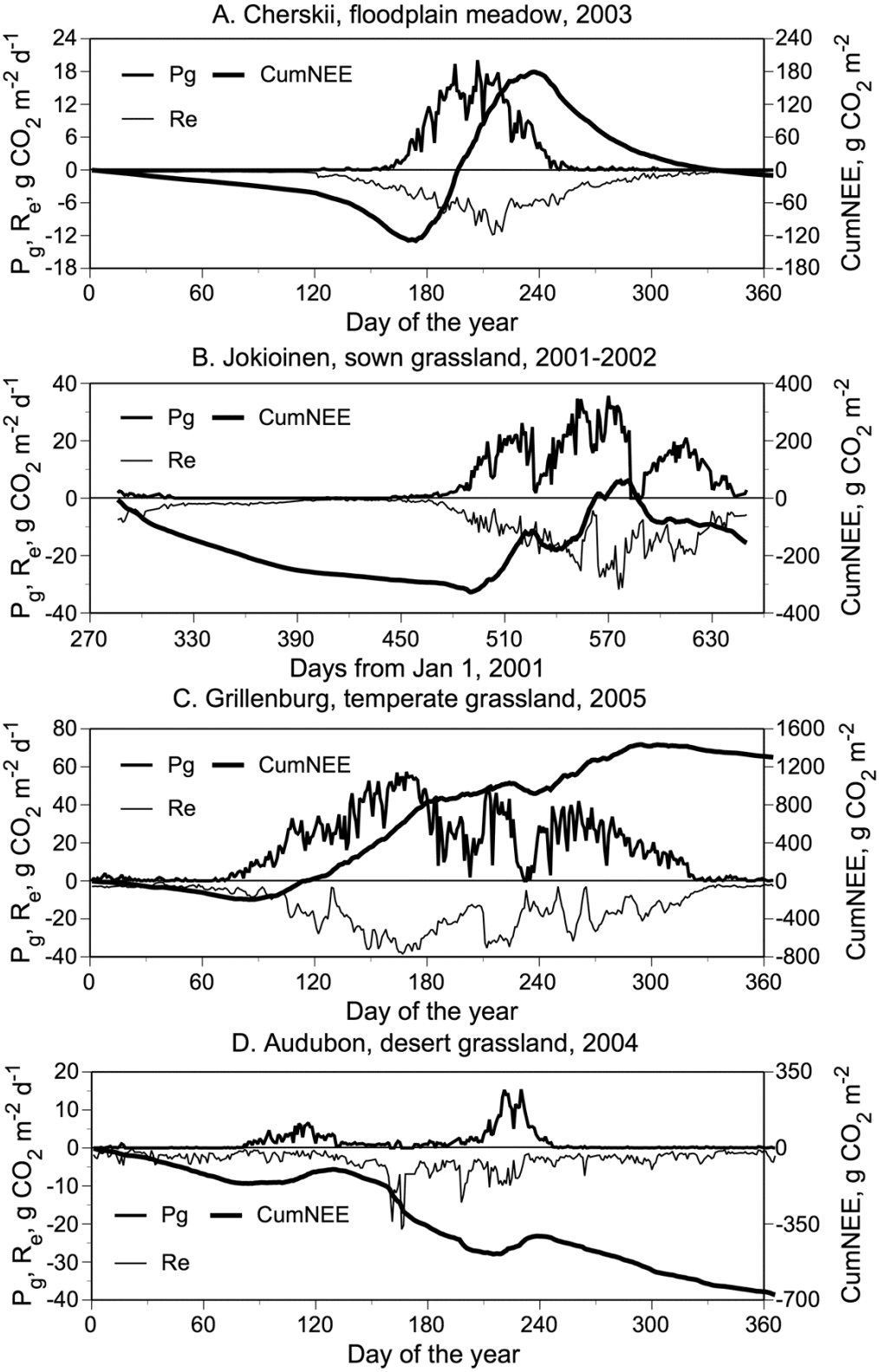
A. Cherskii, floodplain meadow, 2003
Pg
CumNEE
Re
P_g, R_e, g CO_2 m^{-2} d^{-1}
CumNEE, g CO_2 m^{-2}
Day of the year
B. Jokioinen, sown grassland, 2001-2002
Days from Jan 1, 2001
C. Grillenburg, temperate grassland, 2005
D. Audubon, desert grassland, 2004

1

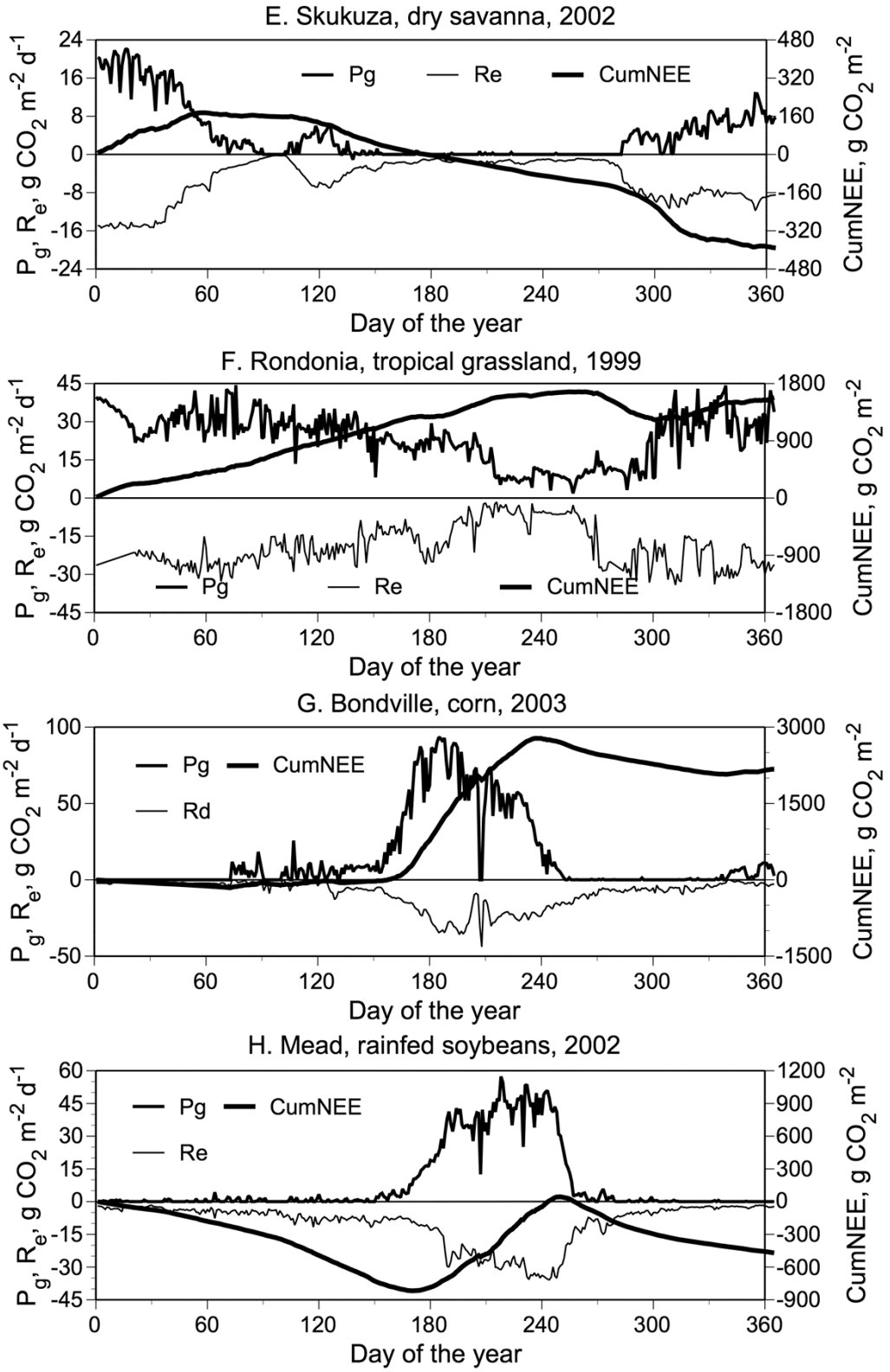
E. Skukuza, dry savanna, 2002
Pg
Re
CumNEE
Day of the year
F. Rondonia, tropical grassland, 1999
Pg
Re
CumNEE
Day of the year
G. Bondville, corn, 2003
Pg
CumNEE
Rd
Day of the year
H. Mead, rainfed soybeans, 2002
Pg
CumNEE
Re
Day of the year
P_g, R_e, g CO_2 m^-2 d^-1
CumNEE, g CO_2 m^-2

Figure 7.

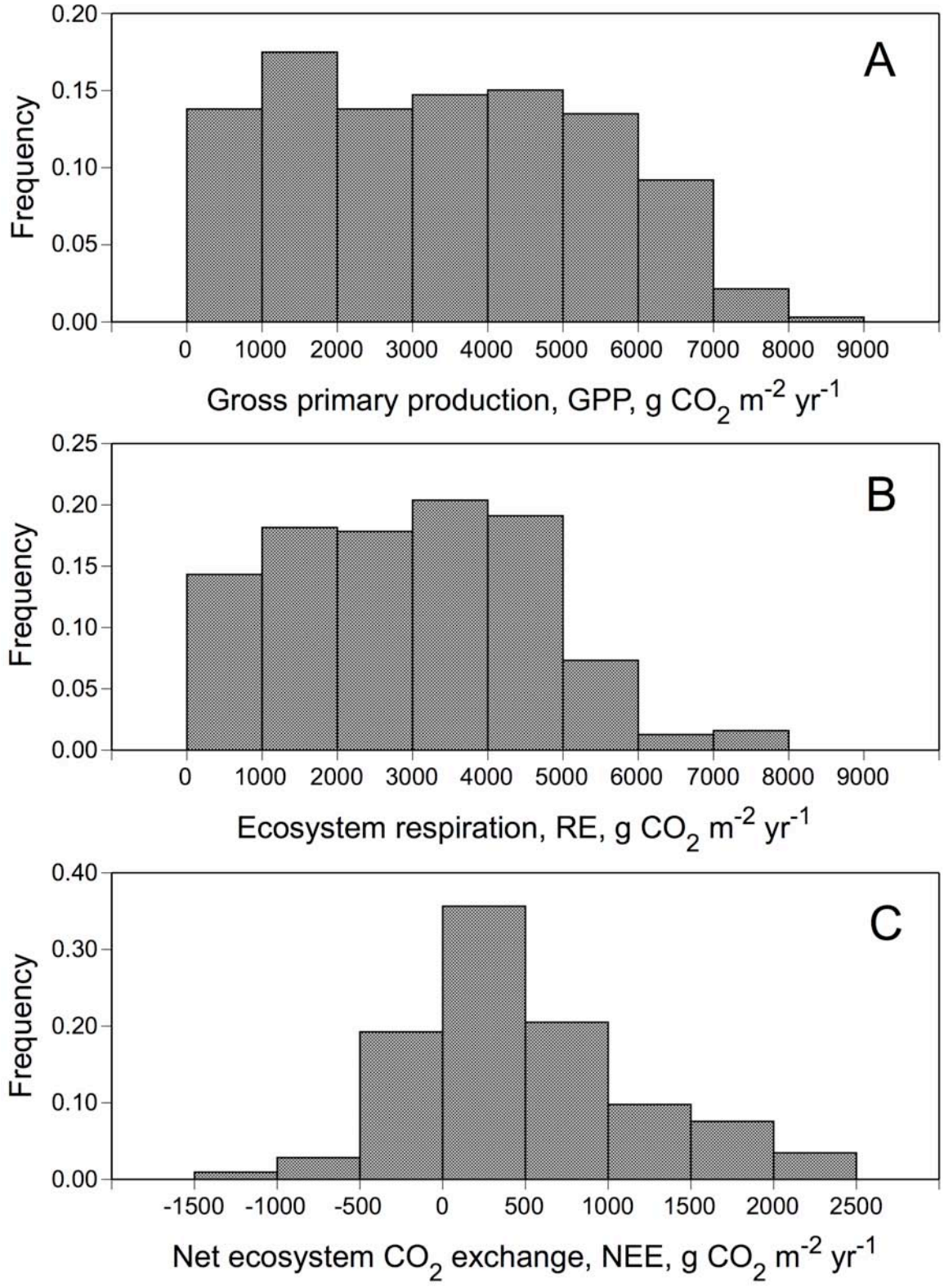
A
Frequency
0.20
0.15
0.10
0.05
0.00
0
1000
2000
3000
4000
5000
6000
7000
8000
9000
Gross primary production, GPP, g CO2 m-2 yr-1
B
Frequency
0.25
0.20
0.15
0.10
0.05
0.00
0
1000
2000
3000
4000
5000
6000
7000
8000
9000
Ecosystem respiration, RE, g CO2 m-2 yr-1
C
Frequency
0.40
0.30
0.20
0.10
0.00
-1500
-1000
-500
0
500
1000
1500
2000
2500
Net ecosystem CO2 exchange, NEE, g CO2 m-2 yr-1

Figure 8.

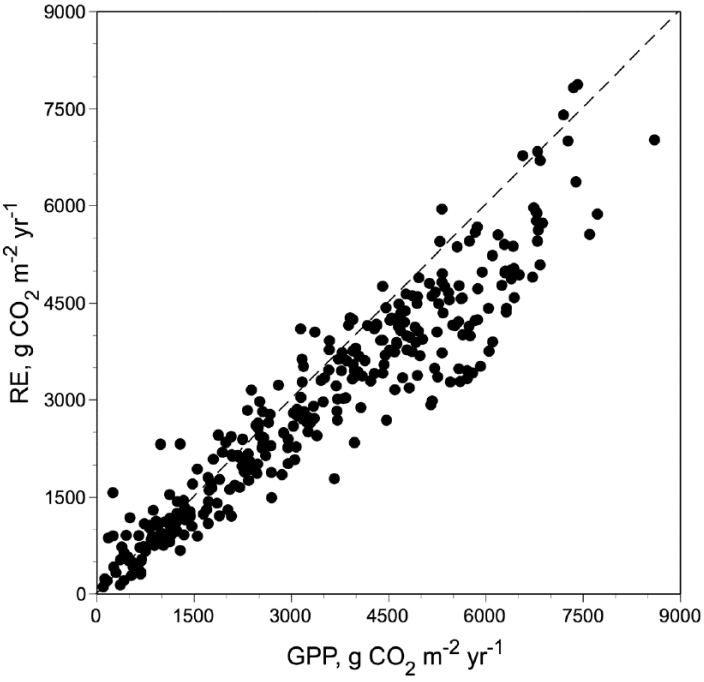
9000
7500
6000
4500
3000
1500
0
RE, g CO2 m-2 yr-1
0
1500
3000
4500
6000
7500
9000
GPP, g CO2 m-2 yr-1

1

2 **Figure 9.**

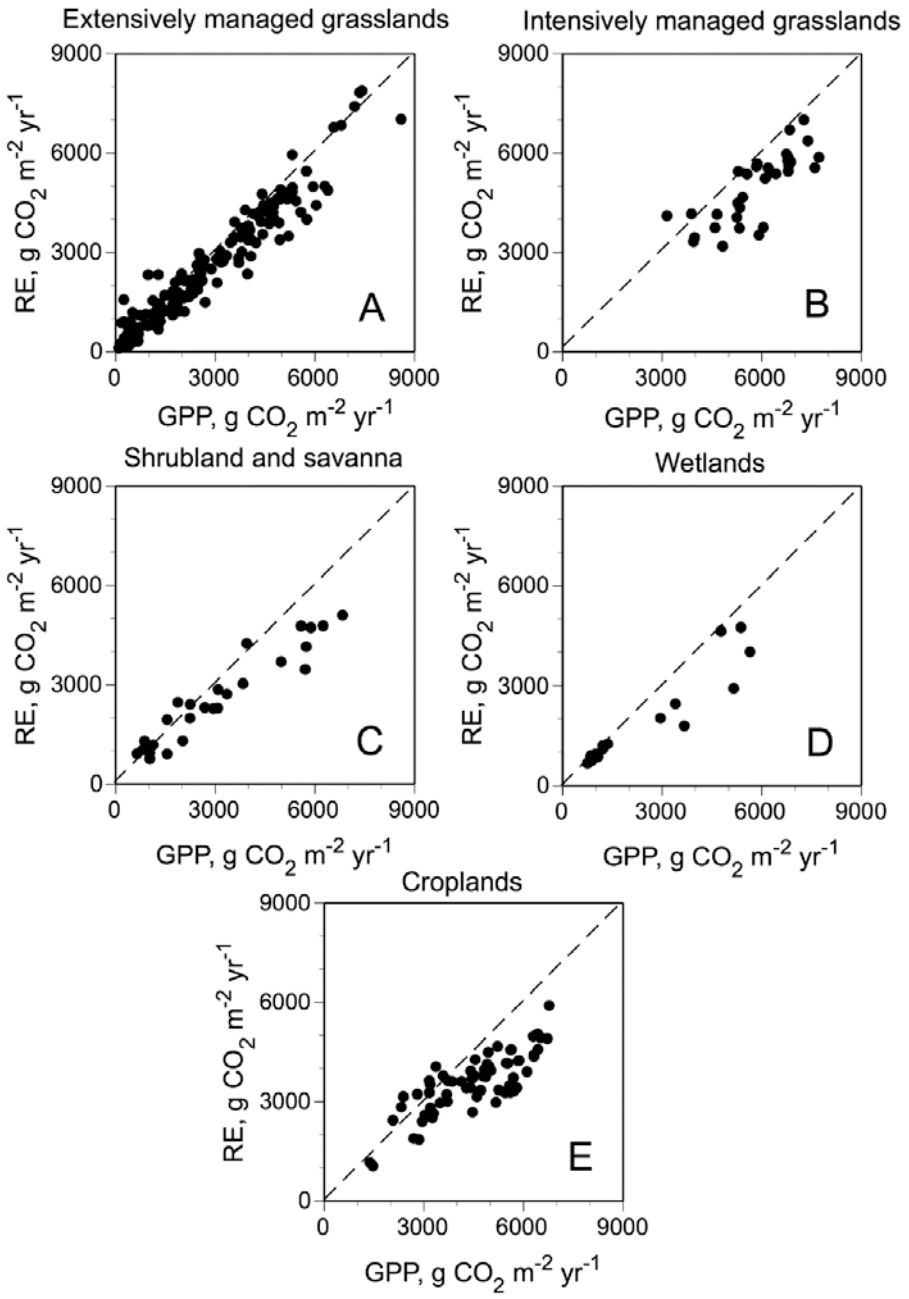
Extensively managed grasslands
Intensively managed grasslands
Shrubland and savanna
Wetlands
Croplands
A
B
C
D
E
RE, g CO2 m-2 yr-1
GPP, g CO2 m-2 yr-1
0
3000
6000
9000

Figure 10.

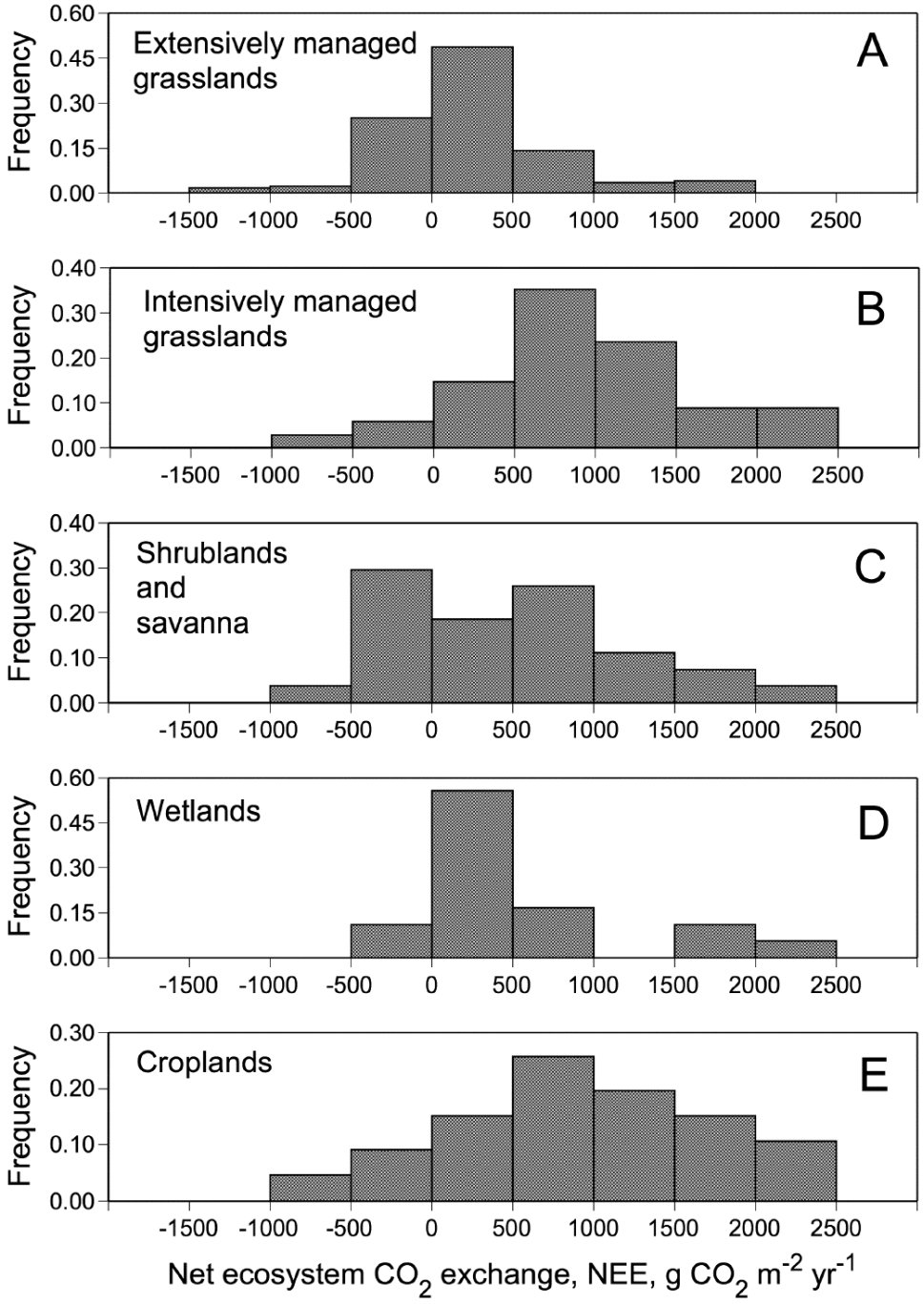
Extensively managed grasslands
A
Intensively managed grasslands
B
Shrublands and savanna
C
Wetlands
D
Croplands
E
Frequency
0.60
0.45
0.30
0.15
0.00
0.40
0.20
0.10
-1500
-1000
-500
0
500
1000
1500
2000
2500
Net ecosystem CO_2 exchange, NEE, g CO_2 m^{-2} yr^{-1}

Figure 11

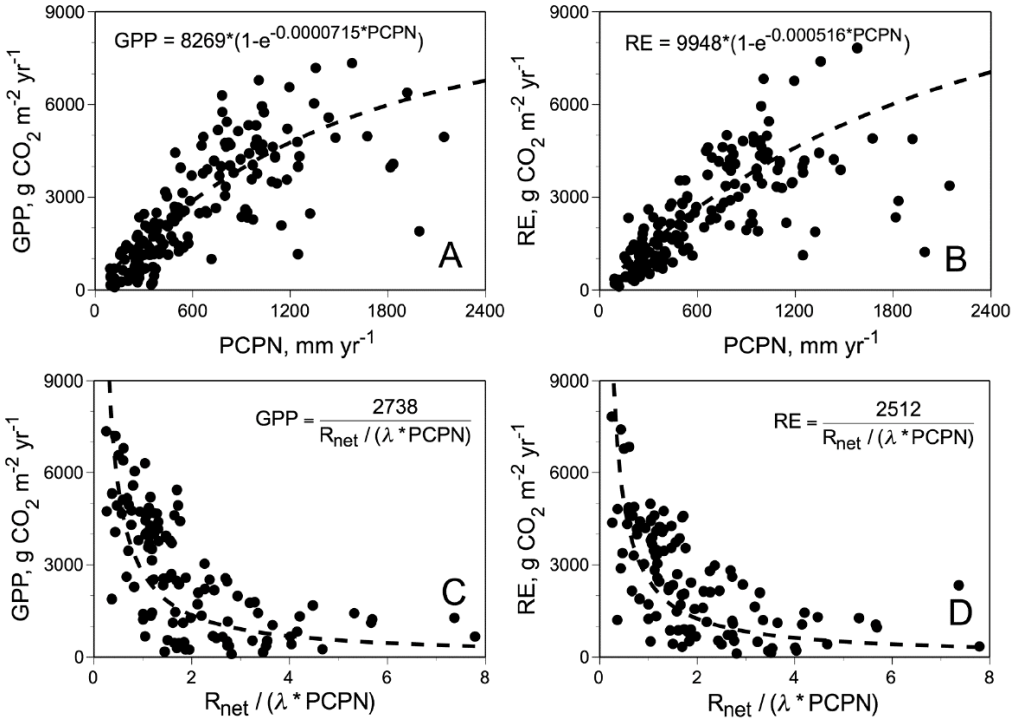

1

2 **Figre 12**

3

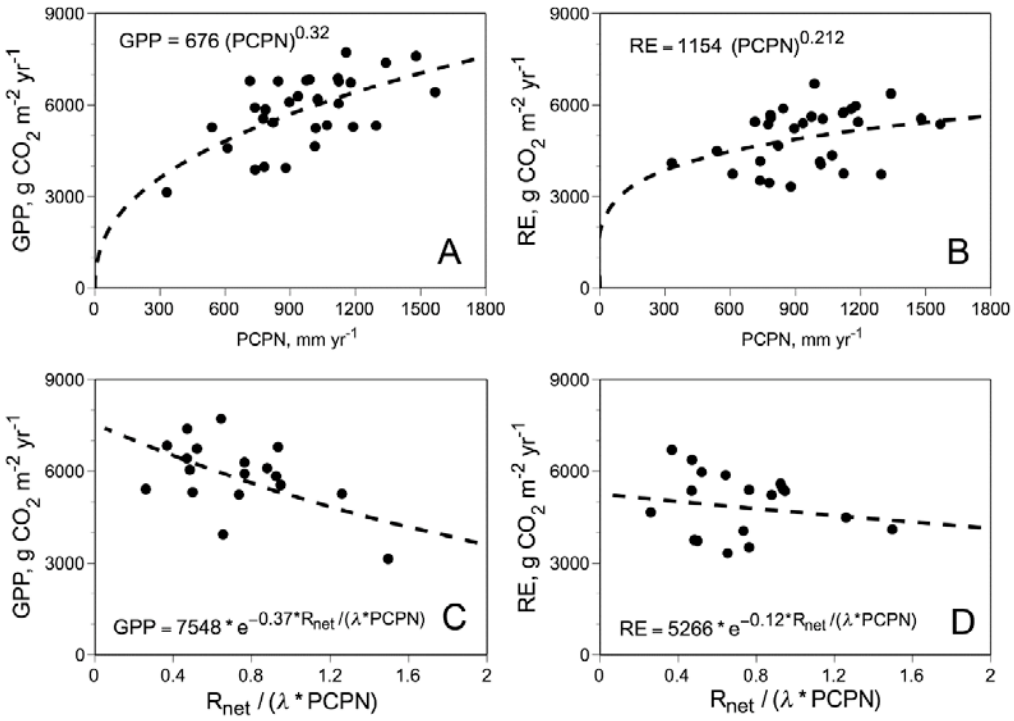

4

5 **Figure 13**

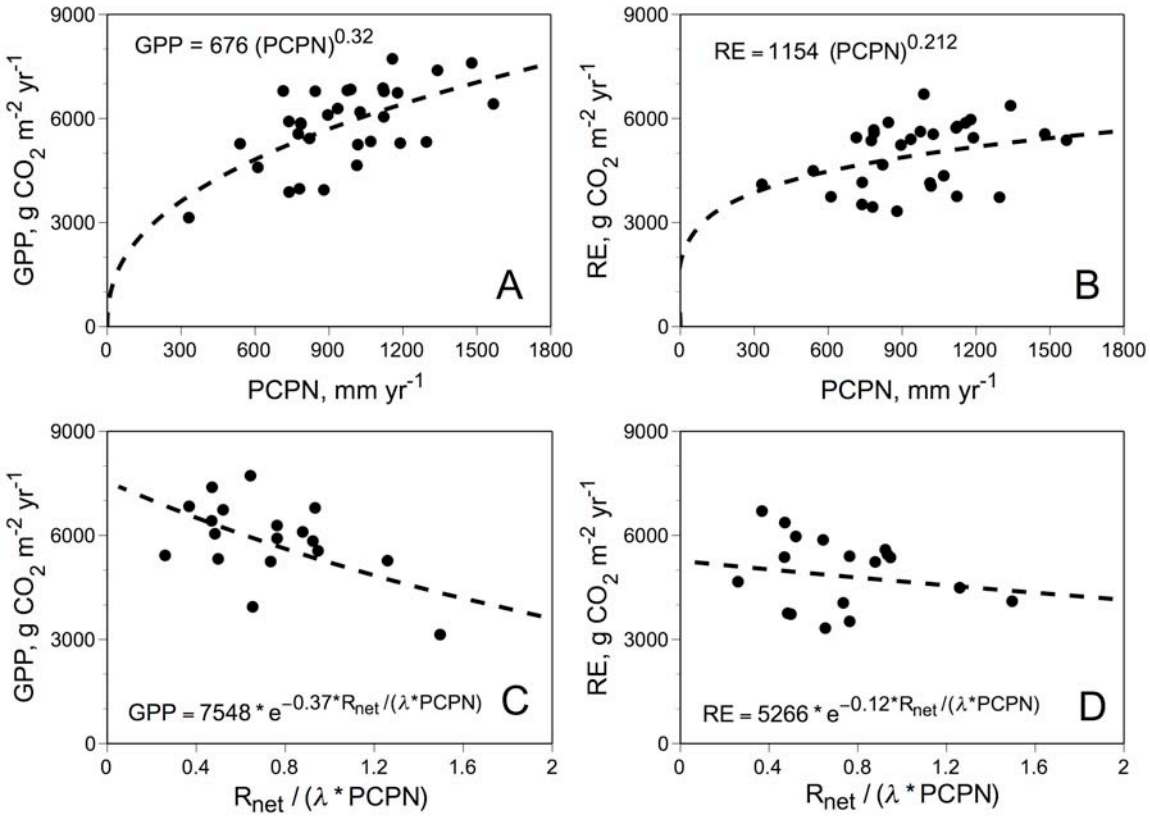

1

2 **Figure 14.**

3